

Study of the proton structure via $\bar{p} p$ annihilation at $\bar{P}ANDA$

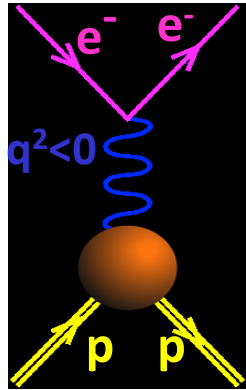
**J. Boucher, M. Gumberidze, T. Hennino,
R. Kunne, D. Marchand, S. Ong, B. Ramstein,
E. Tomasi-Gustafsson, J. Van de Wiele**

Outline

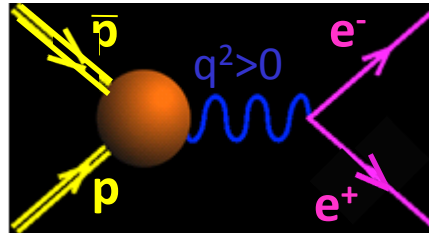
- Motivations: proton electromagnetic form factors
- \overline{P} ANDA detector
- $\overline{p}p \rightarrow e^+e^-$ channel
 - Signal efficiency and background rejection
- $\overline{p}p \rightarrow \pi^0 e^+e^-$ channel
 - Models, first results
- Conclusion & future plans

Proton electromagnetic form factors

Space-like SL



Time-like TL

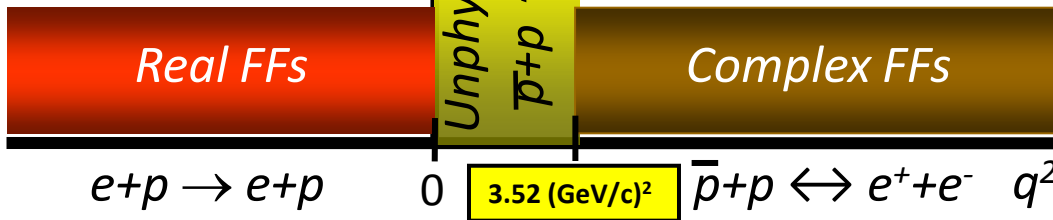


Normalization

- $G_E^p(0)=1$
- $G_M^p(0)=\mu_p$
- $G_E^p(4m_p^2) = G_M^p(4m_p^2)$

Asymptotics

- $|G_{E,M}(q^2)| \sim (q^2)^{-2}$
 - $\frac{G_E}{G_M} \sim \text{real constant}$
- For $q^2 \rightarrow \pm\infty$



• $\lim_{q^2 \rightarrow -\infty} G_{E,M}^{SL}(q^2) = \lim_{q^2 \rightarrow +\infty} G_{E,M}^{TL}(q^2)$ (Phragmén-Lindelöf theorem)

Dispersion relation

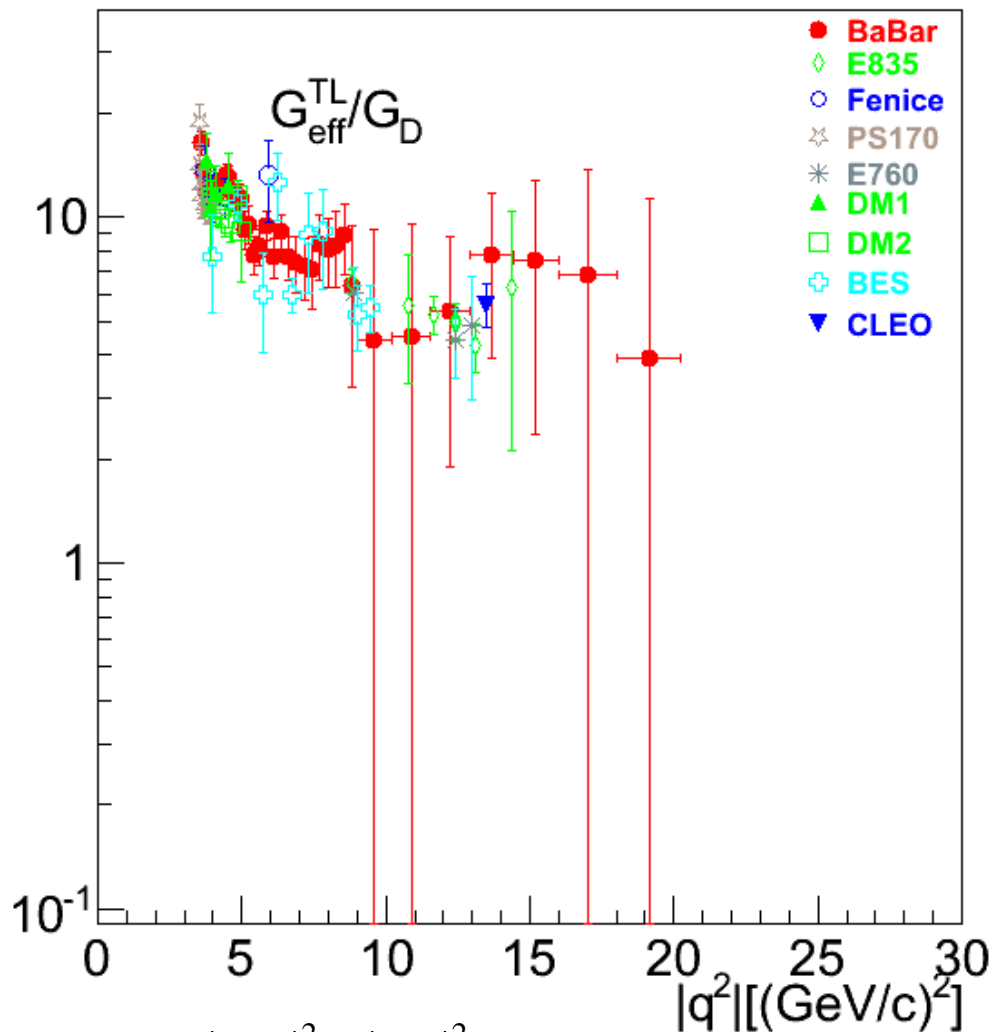
$$G(q^2) = \frac{1}{\pi} \left[\int_{4m_\pi^2}^{4m_p^2} \frac{\text{Im} G(s) ds}{s - q^2} + \int_{4m_p^2}^{\infty} \frac{\text{Im} G(s) ds}{s - q^2} \right]$$

Precise data (SL)

No data (TL)

Low quality data (TL)

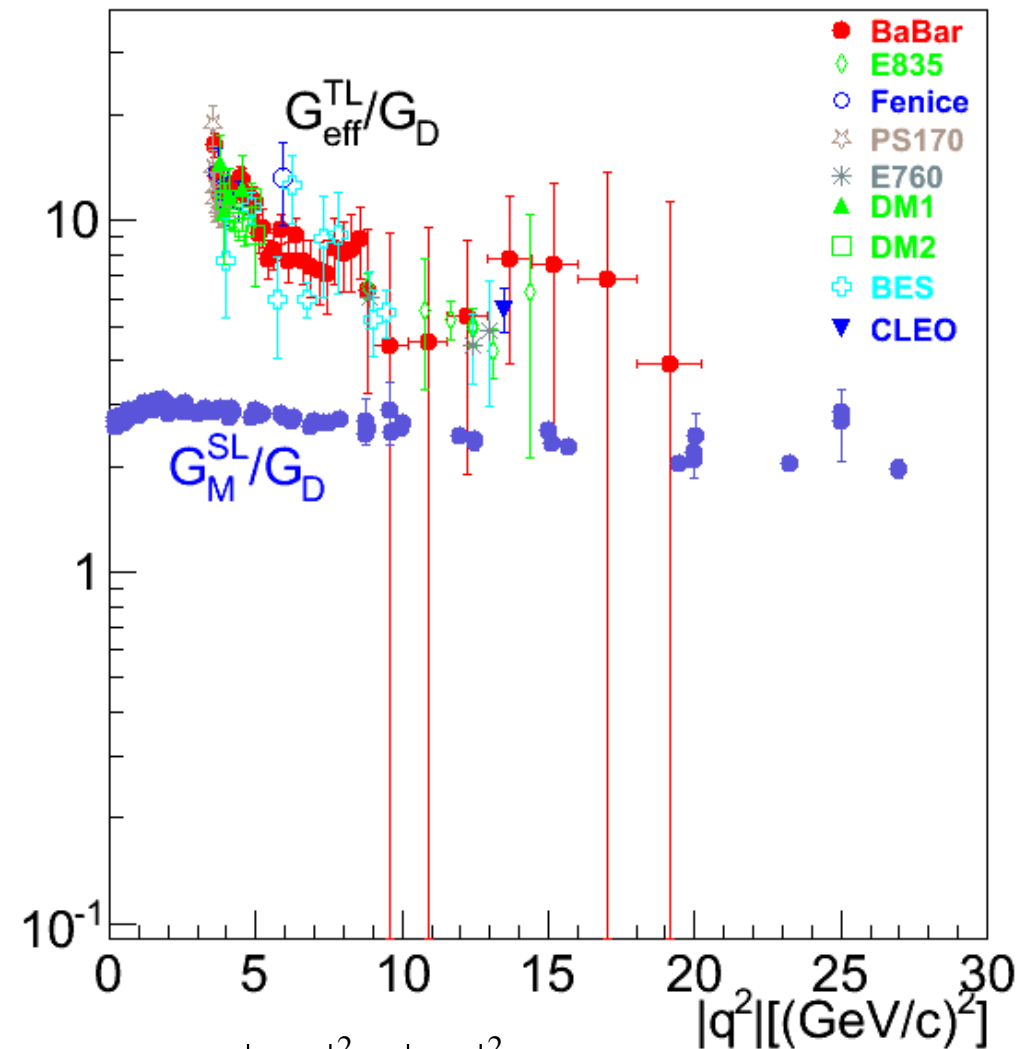
Proton EM form factor data



- TL:**
- $G_{\text{eff}}^{\text{TL}}$ extracted under the assumption $|G_E^{\text{TL}}| = |G_M^{\text{TL}}|$.
 - Few data available at high q^2 .
 - No individual determination of $|G_E^{\text{TL}}|$ and $|G_M^{\text{TL}}|$.

$$G_{\text{eff}}^2 = \frac{2\tau |G_M|^2 + |G_E|^2}{2\tau + 1} \quad G_D = \left(1 + \frac{Q^2}{0.71^2}\right)^{-2}$$

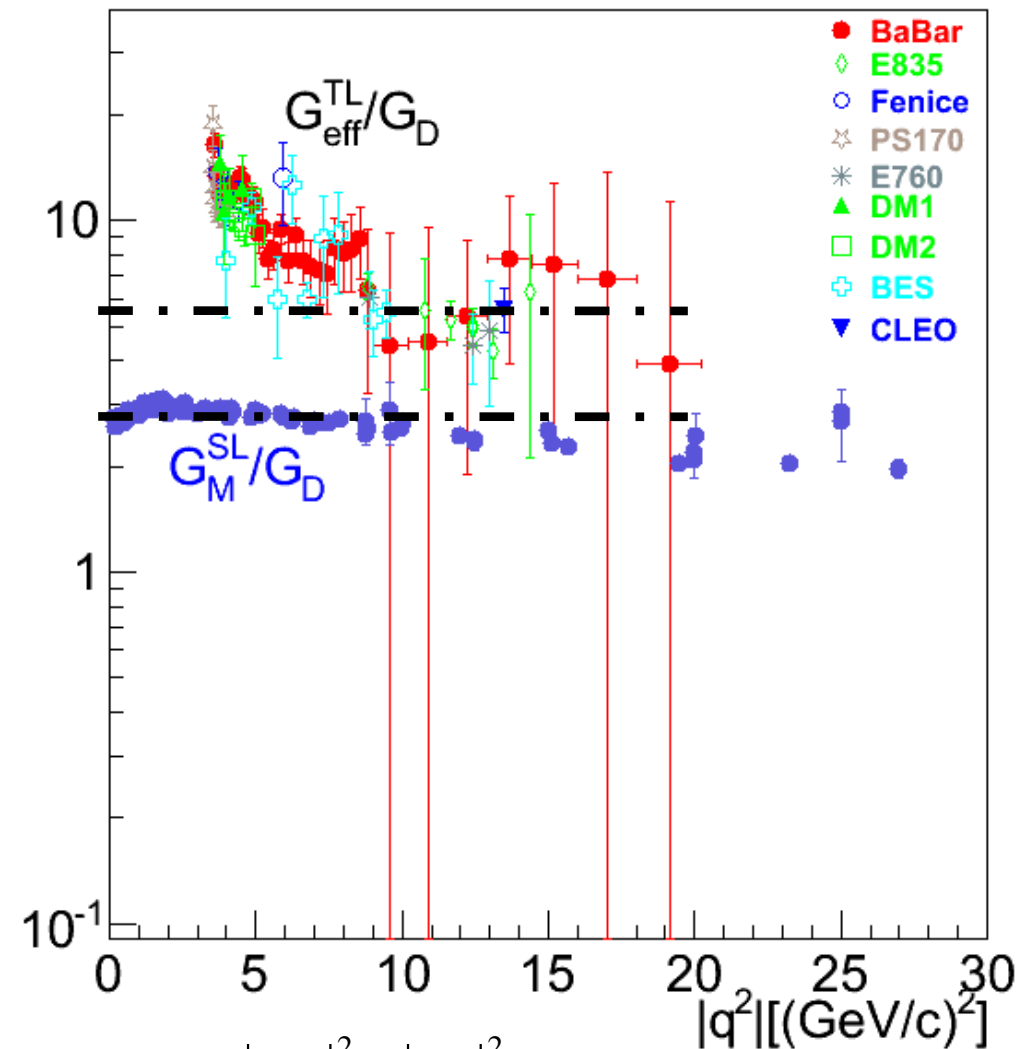
Proton EM form factor data



- TL:** • $G_{\text{eff}}^{\text{TL}}$ extracted under the assumption $|G_E^{\text{TL}}| = |G_M^{\text{TL}}|$.
- Few data available at high q^2 .
 - No individual determination of $|G_E^{\text{TL}}|$ and $|G_M^{\text{TL}}|$.
 - $|G_{\text{eff}}^{\text{TL}}| \approx |G_M^{\text{TL}}| \approx 2 |G_M^{\text{SL}}|$
 \hookrightarrow asymptotic regime not reached

$$|G_{\text{eff}}|^2 = \frac{2\tau |G_M|^2 + |G_E|^2}{2\tau + 1} \quad G_D = \left(1 + \frac{Q^2}{0.71^2}\right)^{-2}$$

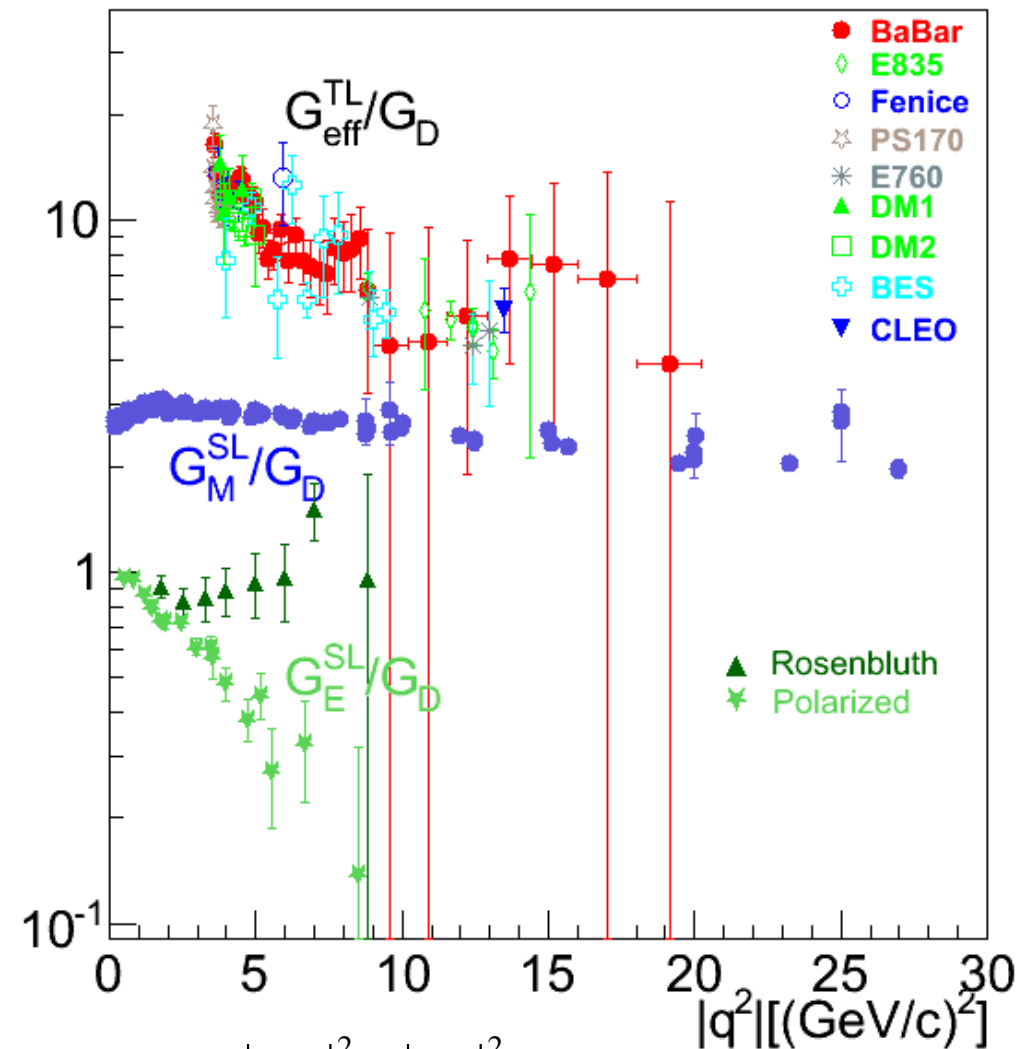
Proton EM form factor data



- TL:** • $G_{\text{eff}}^{\text{TL}}$ extracted under the assumption $|G_E^{\text{TL}}| = |G_M^{\text{TL}}|$.
- Few data available at high q^2 .
 - No individual determination of $|G_E^{\text{TL}}|$ and $|G_M^{\text{TL}}|$.
 - $|G_{\text{eff}}^{\text{TL}}| \approx |G_M^{\text{TL}}| \approx 2 |G_M^{\text{SL}}|$
 \hookrightarrow asymptotic regime not reached

$$|G_{\text{eff}}|^2 = \frac{2\tau |G_M|^2 + |G_E|^2}{2\tau + 1} \quad G_D = \left(1 + \frac{Q^2}{0.71^2}\right)^{-2}$$

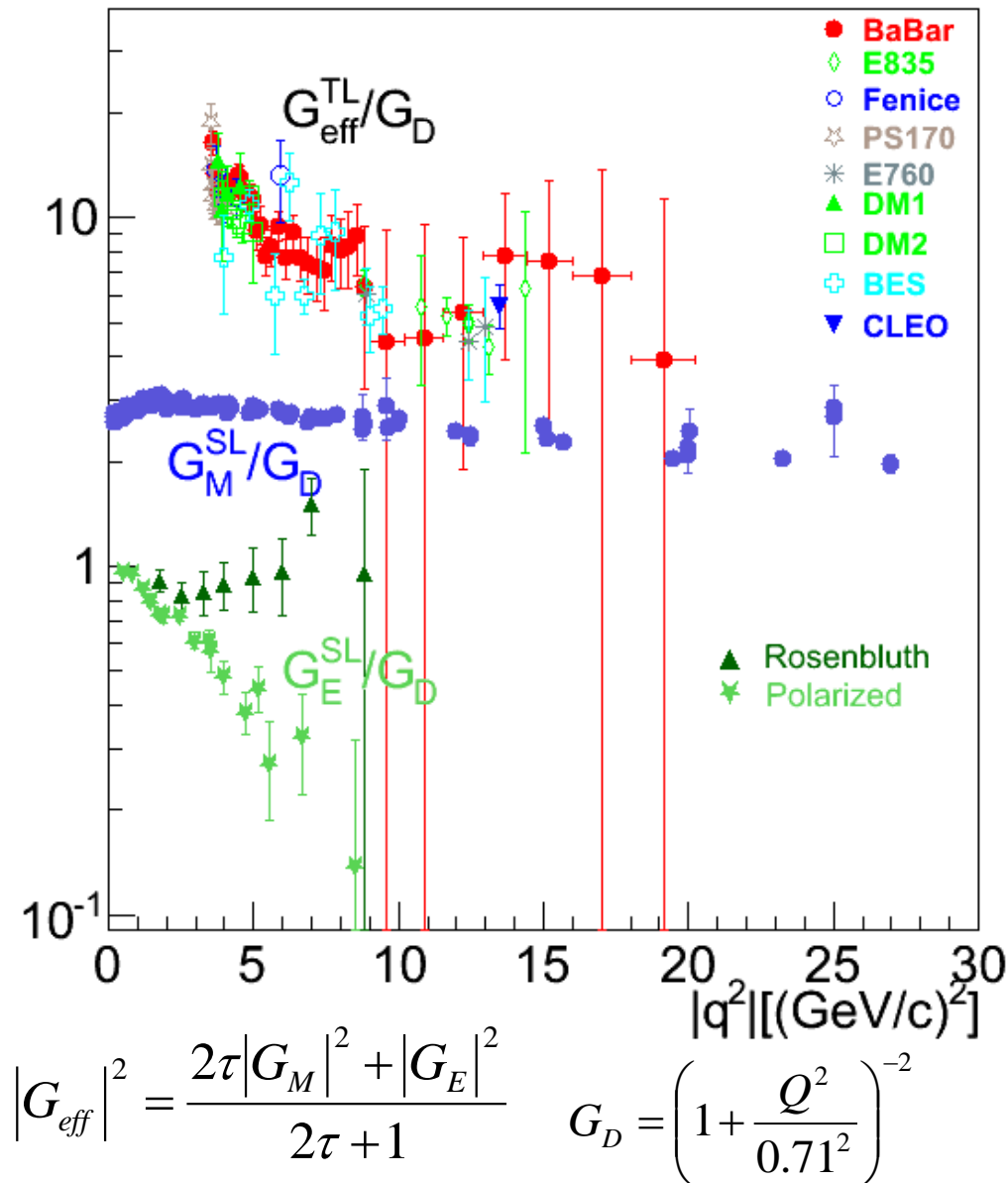
Proton EM form factor data



$$|G_{eff}|^2 = \frac{2\tau |G_M|^2 + |G_E|^2}{2\tau + 1} \quad G_D = \left(1 + \frac{Q^2}{0.71^2}\right)^{-2}$$

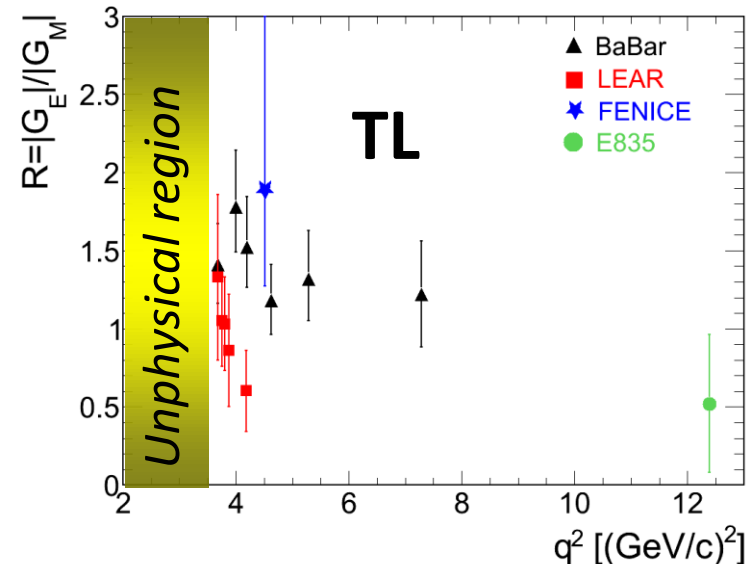
- TL:**
- G_{eff}^{TL} extracted under the assumption $|G_E^{TL}| = |G_M^{TL}|$.
 - Few data available at high q^2 .
 - No individual determination of $|G_E^{TL}|$ and $|G_M^{TL}|$.
 - $|G_{eff}^{TL}| \approx |G_M^{TL}| \approx 2 |G_M^{SL}|$
 \hookrightarrow asymptotic regime not reached
- SL:**
- Contradictory results from the Rosenbluth and the recoil proton polarization methods.

Proton EM form factor data

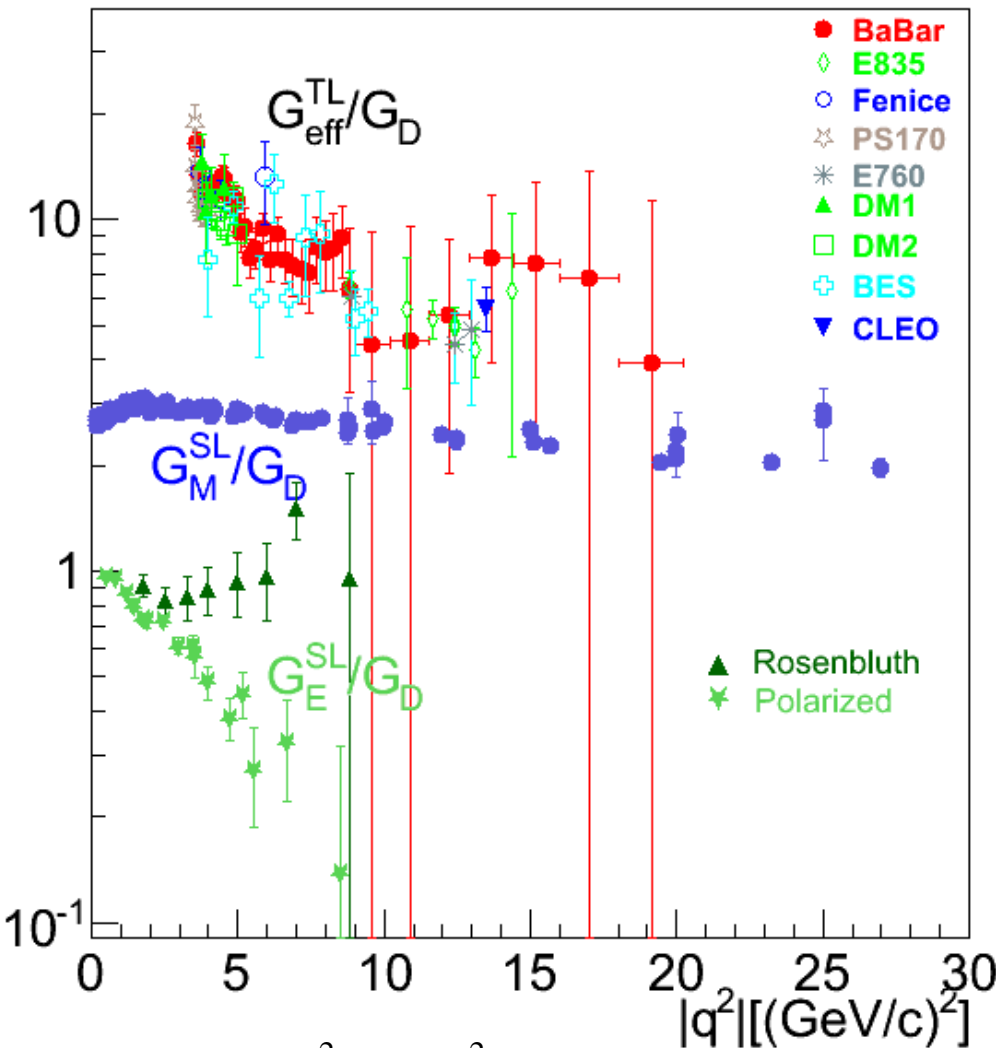


- TL:**
- G_{eff}^{TL} extracted under the assumption $|G_E^{TL}| = |G_M^{TL}|$.
 - Few data available at high q^2 .
 - No individual determination of $|G_E^{TL}|$ and $|G_M^{TL}|$.
 - $|G_{eff}^{TL}| \approx |G_M^{TL}| \approx 2 |G_M^{SL}|$
 \hookrightarrow asymptotic regime not reached

- SL:**
- Contradictory results from the Rosenbluth and the recoil proton polarization methods.

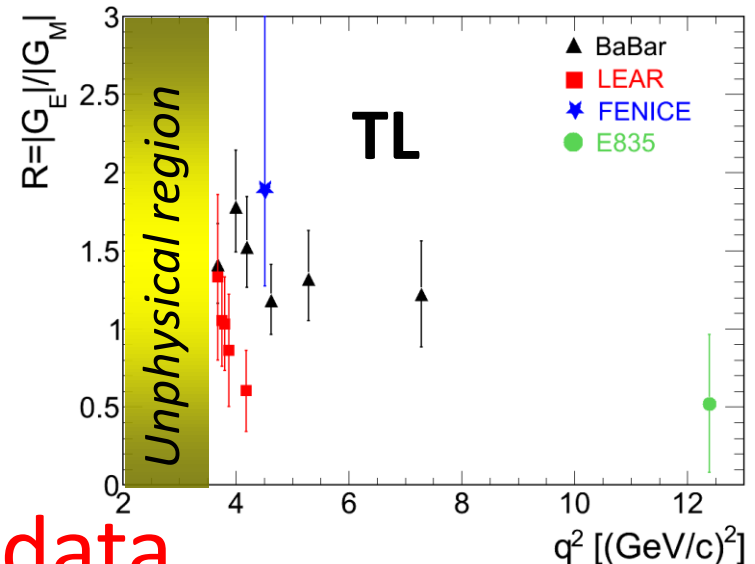


Proton EM form factor data



- TL:**
- $G_{\text{eff}}^{\text{TL}}$ extracted under the assumption $|G_E^{\text{TL}}| = |G_M^{\text{TL}}|$.
 - Few data available at high q^2 .
 - No individual determination of $|G_E^{\text{TL}}|$ and $|G_M^{\text{TL}}|$.
 - $|G_{\text{eff}}^{\text{TL}}| \approx |G_M^{\text{TL}}| \approx 2 |G_M^{\text{SL}}|$
 \hookrightarrow asymptotic regime not reached

- SL:**
- Contradictory results from the Rosenbluth and the recoil proton polarization methods.



Need for precise data

FAIR, Facility for Antiproton and Ion Research, Darmstadt, Germany



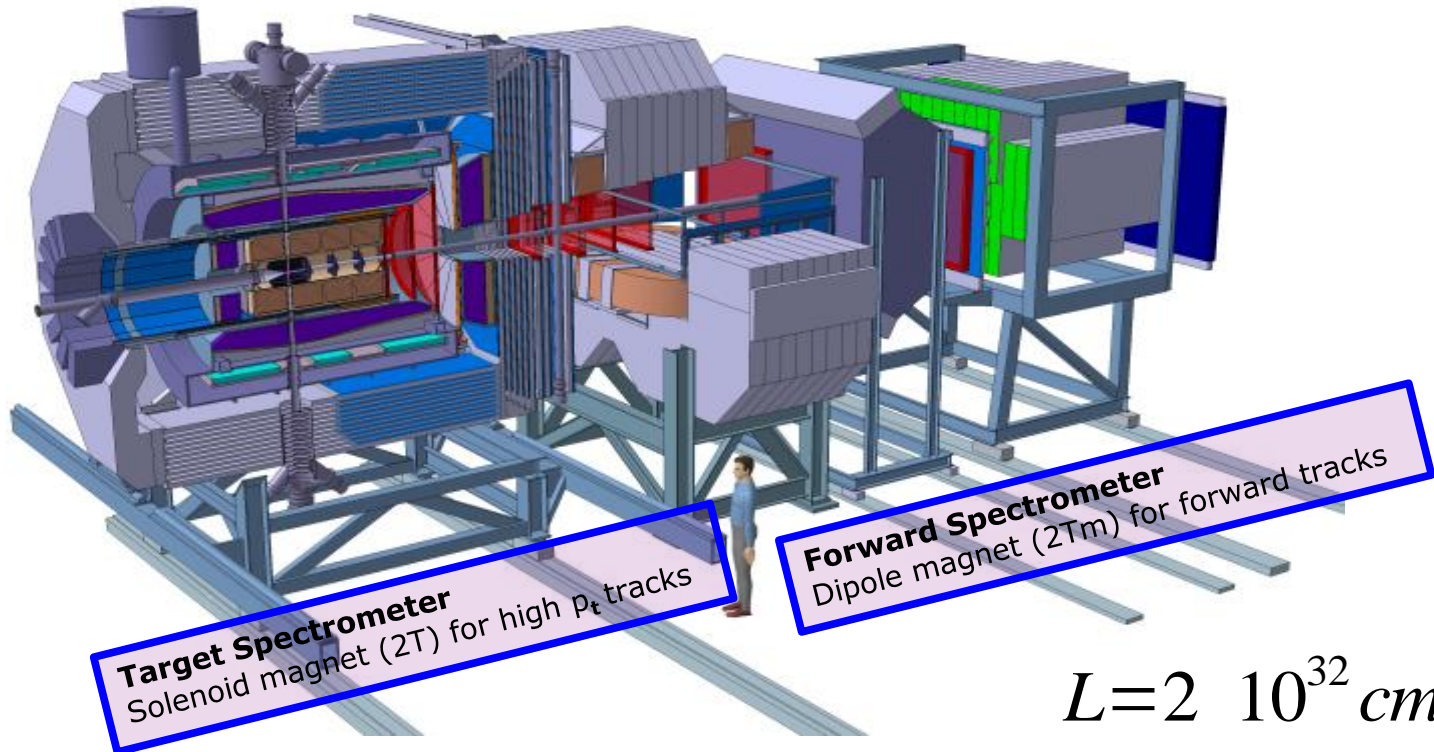
GSI, Darmstadt

- heavy ion physics
- nuclear structure
- atomic and plasma physics

FAIR, Darmstadt: New facility

- heavy ion physics & nuclear structure
- atomic, plasma and applied physics
- higher intensities & energies
- **antiproton physics**

PANDA detector



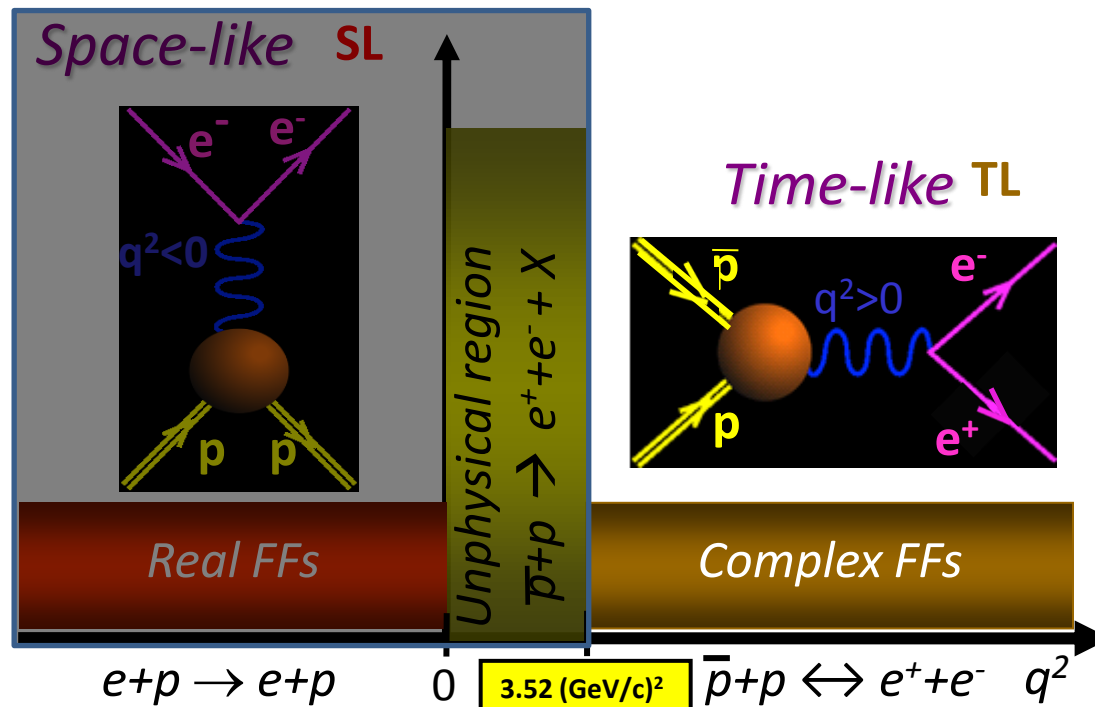
$$L=2 \cdot 10^{32} \text{ cm}^{-2} \text{ s}^{-1}$$

Detector requirements:

- nearly 4π solid angle;
- high rate capability: $2 \cdot 10^7$ interactions/s;
- efficient event selection;
- good momentum resolution $\Delta p/p \approx 1\%$ at 1 GeV/c;
- vertex resolution $< 100 \mu\text{m}$ for $K^0, \Sigma, \Lambda, (D^\pm, c\tau \approx 317 \mu\text{m})$;
- good PID ($\gamma, e, \mu, \pi, K, p$): dE/dx, Cerenkov, calorimetry, muons;
- γ detection: few MeV $< E_\gamma < 10$ GeV.

Simulation studies of $\bar{p} p \rightarrow e^+ e^-$

- Sensitivity to $|G_E|$ and $|G_M|$
- Background suppression



Sensitivity to $|G_E|$ and $|G_M|$

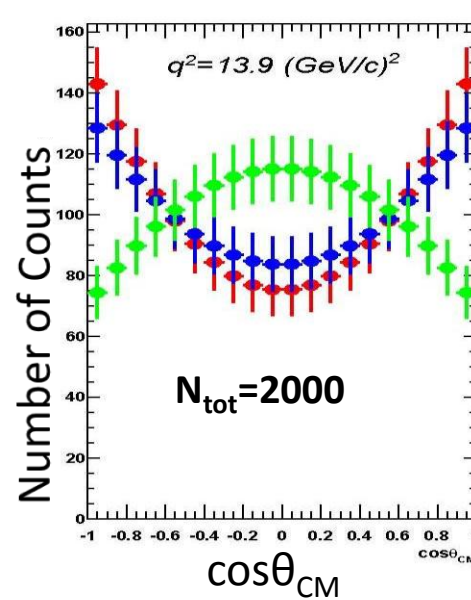
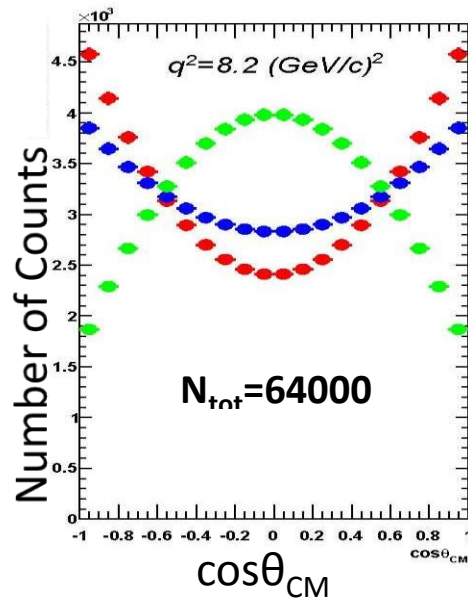
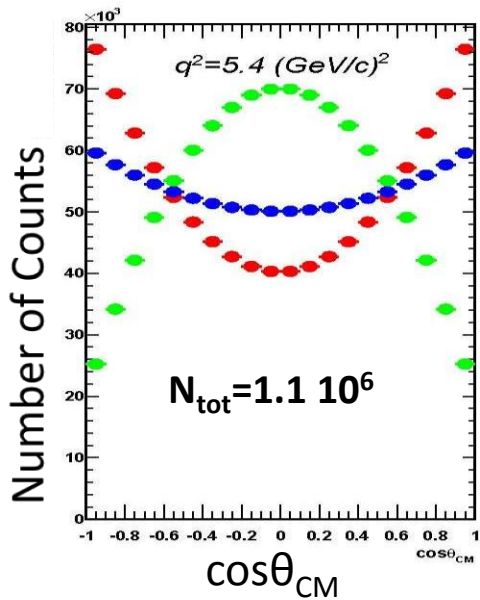
General expression for the differential cross section: $d^n \sigma \propto |M|^2 \propto L^{\mu\nu} H_{\mu\nu}(s, G_E, G_M)$

$$\frac{d\sigma}{d(\cos \theta_{CM})} = \frac{\pi(\alpha \hbar c)^2}{8m_p^2 \sqrt{\tau(\tau-1)}} \left[|G_M^{TL}|^2 (1 + \cos^2 \theta_{CM}) + \frac{1}{\tau} |G_E^{TL}|^2 \sin^2 \theta_{CM} \right] \quad \tau = \frac{q^2}{4m_p^2}$$



Direct access to $|G_E|$ and $|G_M|$ via the lepton angular distribution

Bin size=0.1



$$|G_E| = 0$$

$$|G_E| = |G_M|$$

$$|G_E| = 3 |G_M|$$

$$\mathcal{L}_{\text{int}} = 2 \text{ fb}^{-1}$$

Background suppression

Background reactions

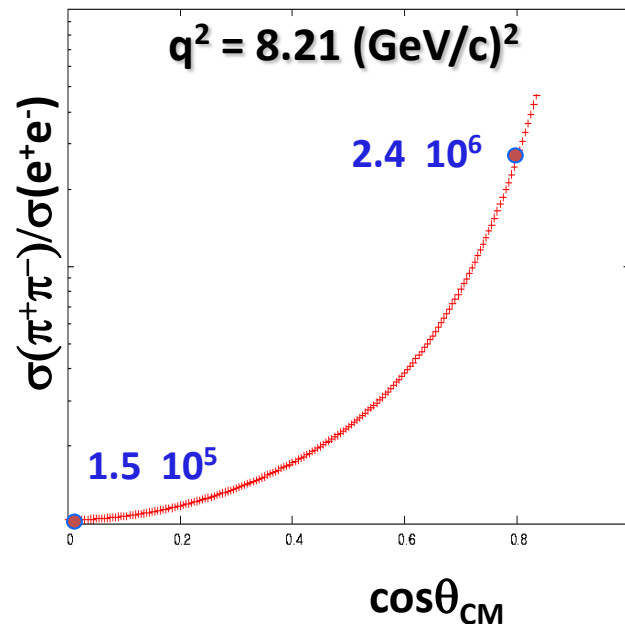
Dominated by 2-charged body reactions

(e.g.: $\bar{p}p$, $\pi^+\pi^-$, $\mu^+\mu^-$, K^+K^-)

Most difficult background to suppress is $\pi^+\pi^-$,

→ PID (Calorimeters, dE/dx , DIRC),

→ Kinematical correlation $p=f(\theta)$.

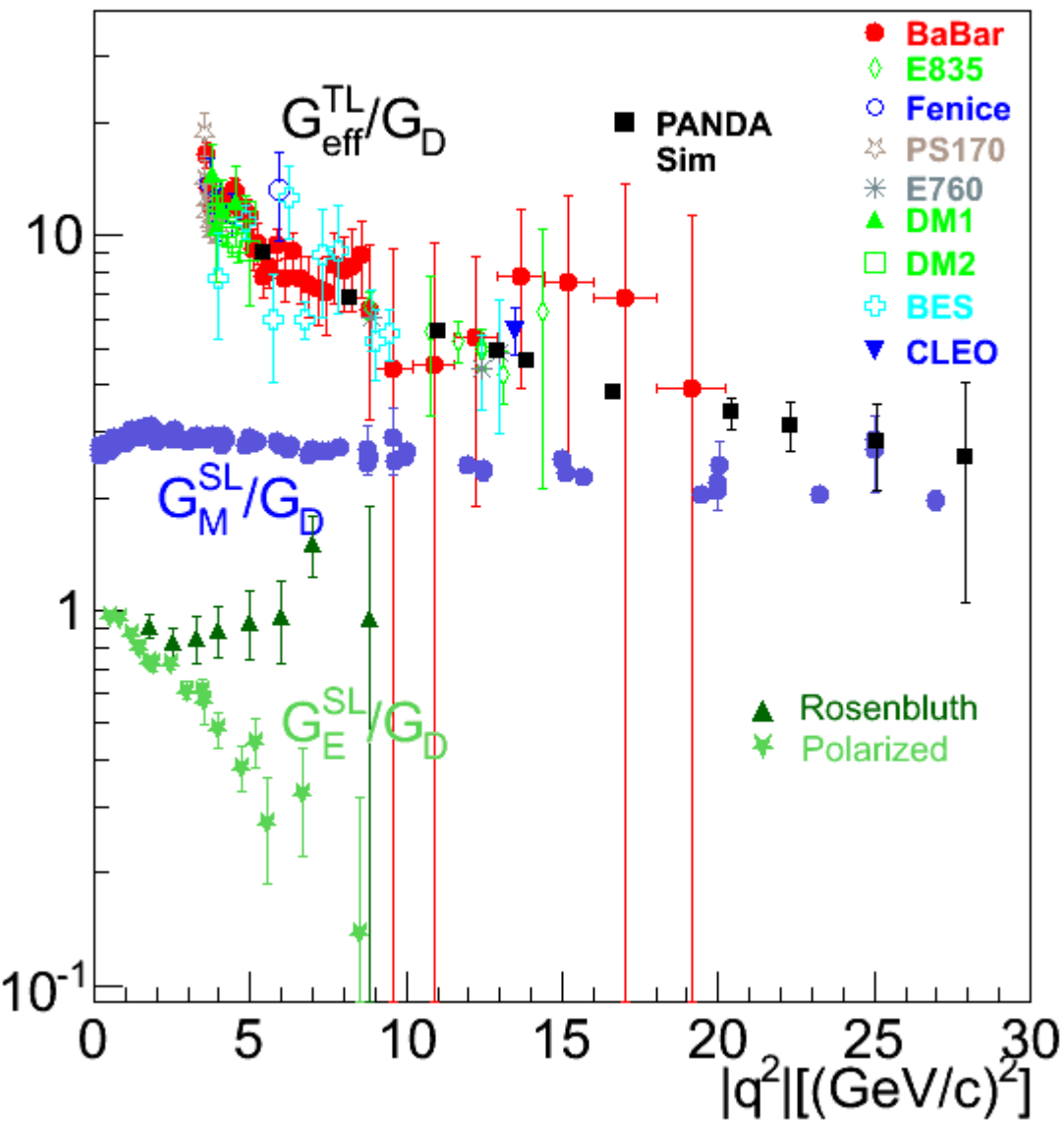


*Background suppression factor
is at least of the order of 10^9
taking into account
PID & kinematic fit !!*

q^2 [GeV/c] ²	$\pi^+\pi^-$ contamination
8.2	0.004 %
12.9	0.017 %
16.7	0.061 %

M. Sudol et al., Eur. Phys. J. A44, 373-384, 2010

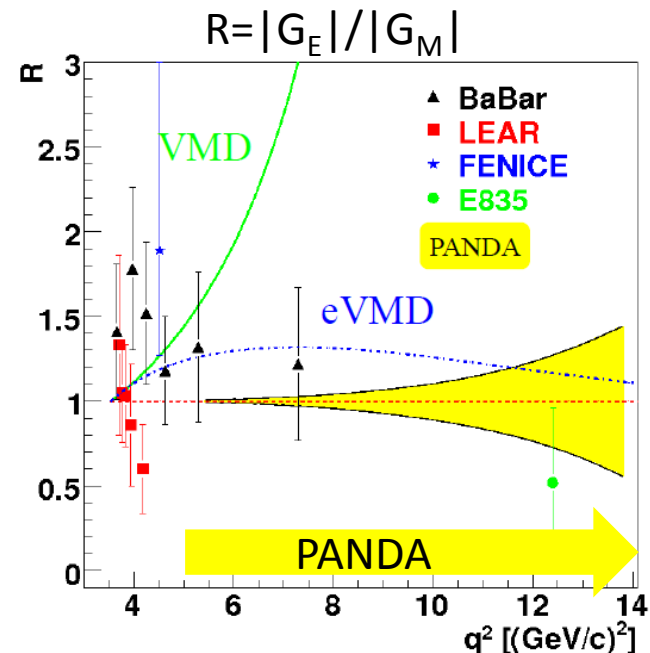
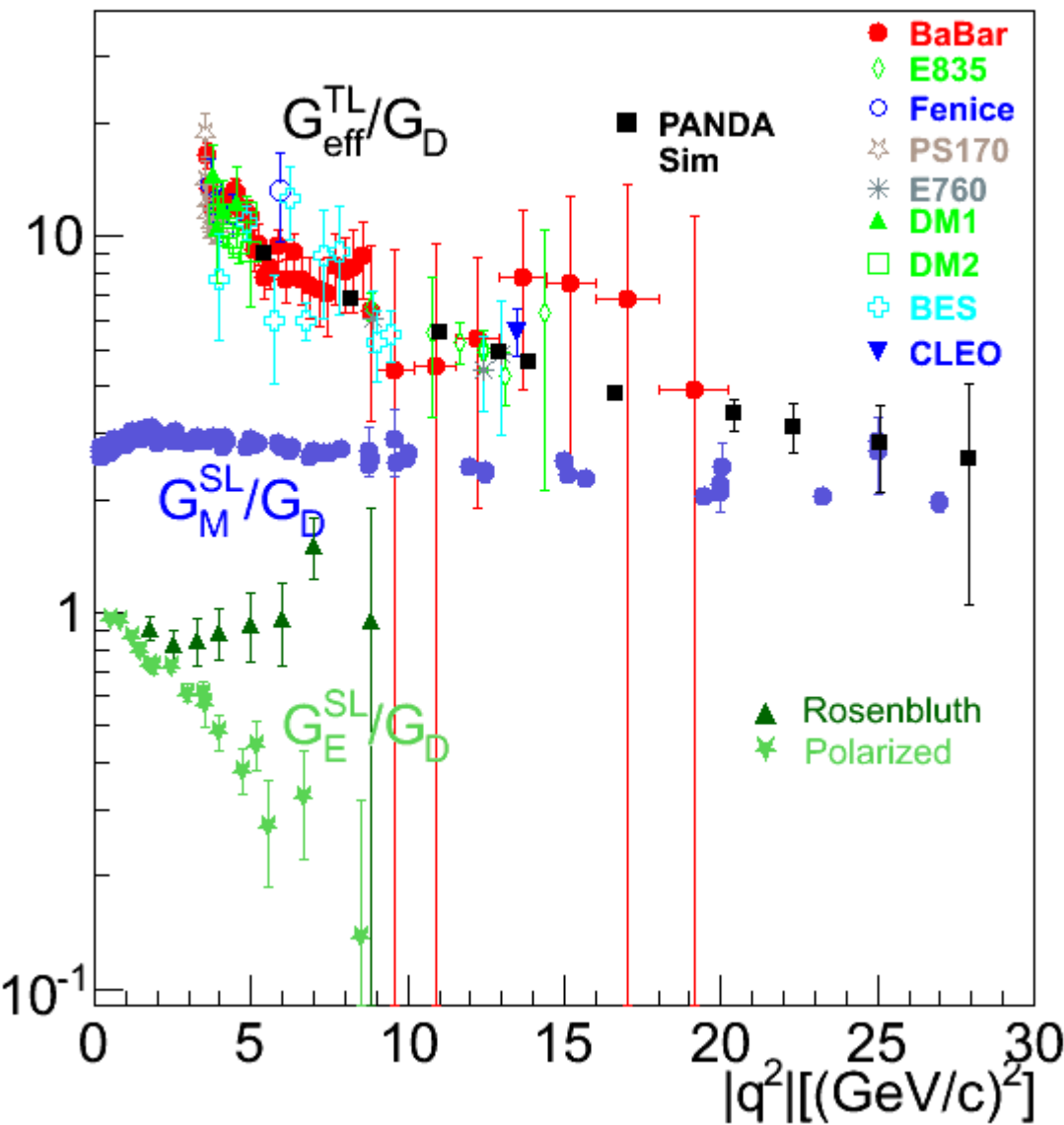
Expected precision with \bar{P} ANDA



$$G_D = \left(1 + \frac{Q^2}{0.71^2}\right)^{-2}$$

$$|G_{eff}|^2 = \frac{2\tau |G_M|^2 + |G_E|^2}{2\tau + 1}$$

Expected precision with $\bar{\text{P}}\text{ANDA}$



PANDA:

→ Separated determination of $|G_E^{\text{TL}}|$ and $|G_M^{\text{TL}}|$ up to 14 (GeV/c)^2

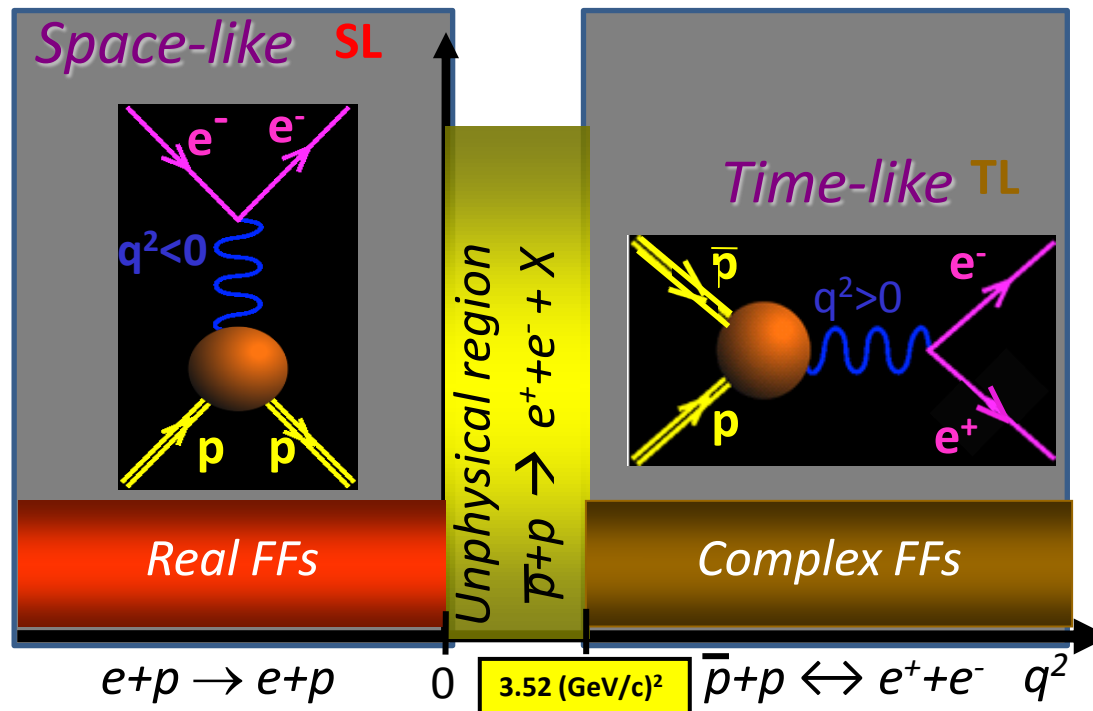
→ Measurement of $|G_{\text{eff}}^{\text{TL}}|$ at higher q^2

$$G_D = \left(1 + \frac{Q^2}{0.71^2}\right)^{-2}$$

$$|G_{\text{eff}}^{\text{TL}}|^2 = \frac{2\tau |G_M^{\text{TL}}|^2 + |G_E^{\text{TL}}|^2}{2\tau + 1}$$

Simulation studies of $\bar{p} p \rightarrow \pi^0 e^+ e^-$

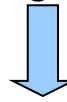
- Models
- Simulations



Form factors in the unphysical region

M. P. Rekalo, Sov. J. Nucl. Phys., vol1, 760 (1965)

Access the proton electromagnetic form factors in TL region



Form factor parametrizations

pQCD inspired :

$$|G_E^p| = |G_M^p| = \frac{98 \text{ GeV}^4}{q^4 \left(\ln^2 \frac{q^2}{\Lambda^2} + \pi^2 \right)}$$

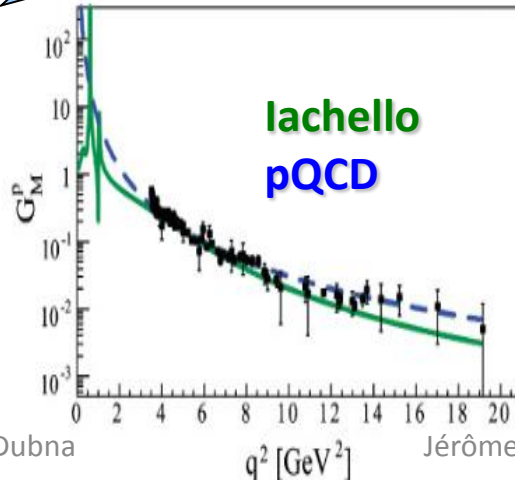
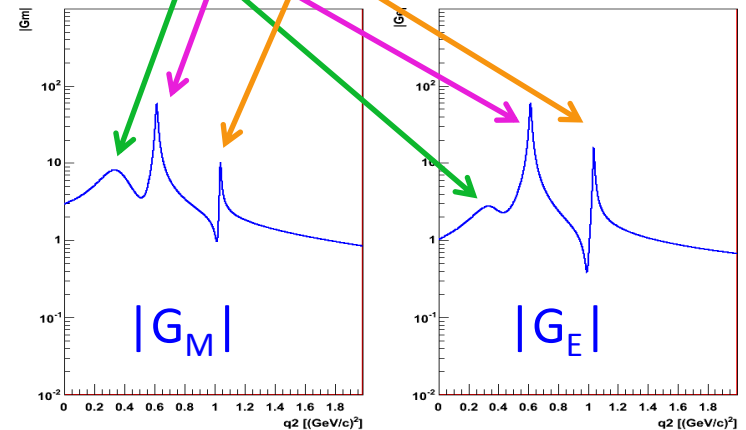
$$q^2 > \Lambda^2 = 0.3^2 (\text{GeV} / c)^2$$



Vector Meson Dominance (VMD):

➤ F. Iachello, Phys. Rev. C69, 055204, 2004

ρ , ω and ϕ resonances



C. Adamuřcin et al.
Phys. Rev. C 75,
045205, 2007

Feasibility

Starting point:

C. Adamuščín, E.A. Kuraev, E. Tomasi-Gustafsson, F. Maas, Phys. Rev. C 75, 045205, 2007

Cross sections ($s=8.21\text{GeV}^2$):

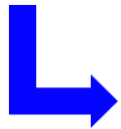
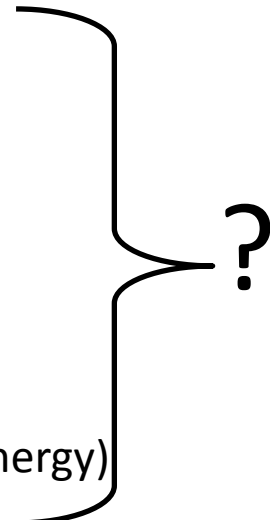
$$\sigma(\bar{p}p \rightarrow \pi^0 e^+ e^-) : \sigma(\bar{p}p \rightarrow \pi \pi \pi) = 1 : 600$$

(Adamuščín with VMD) (data)

From feasibility study of ($\bar{p}p \rightarrow e^+ e^-$):

$$\sigma(\bar{p}p \rightarrow e^+ e^-) : \sigma(\bar{p}p \rightarrow \pi \pi) = 1 : 10^6$$

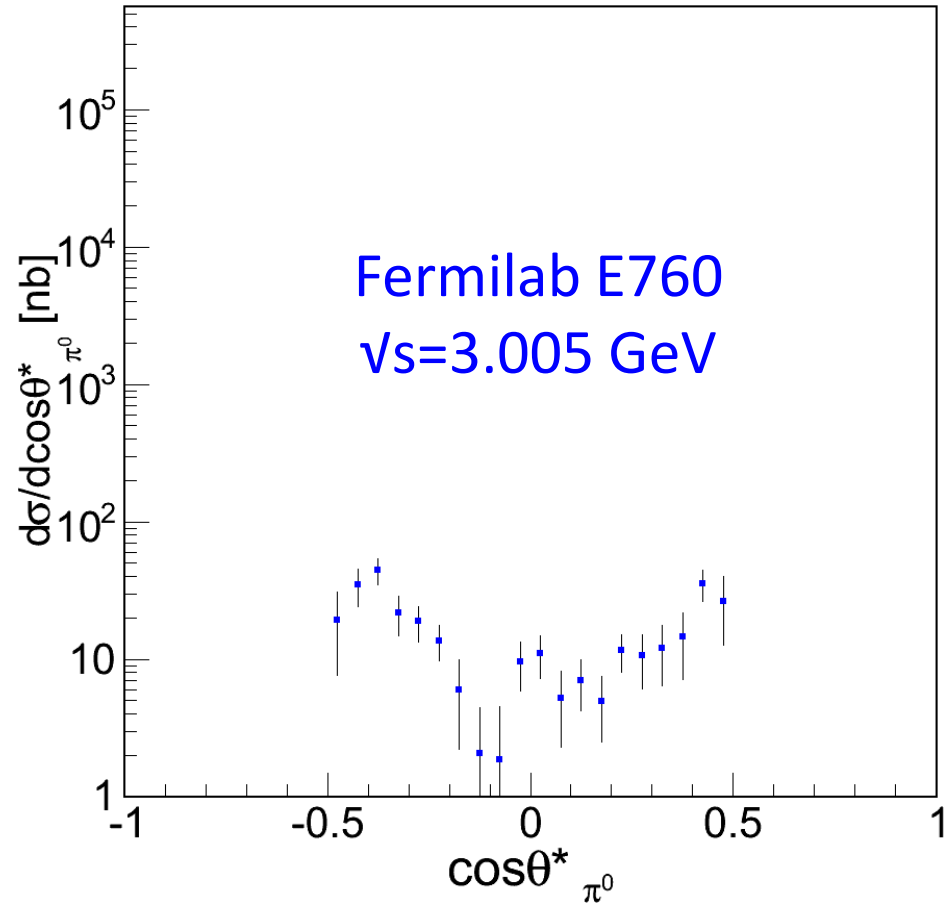
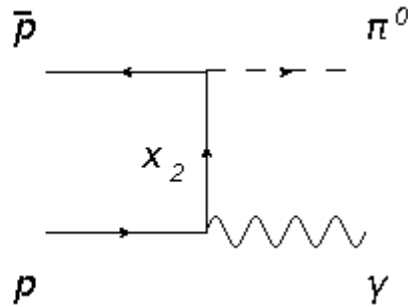
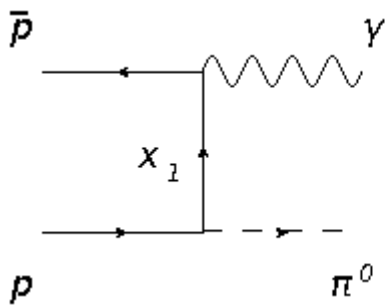
(almost independent on energy)



Need to constrain model by data

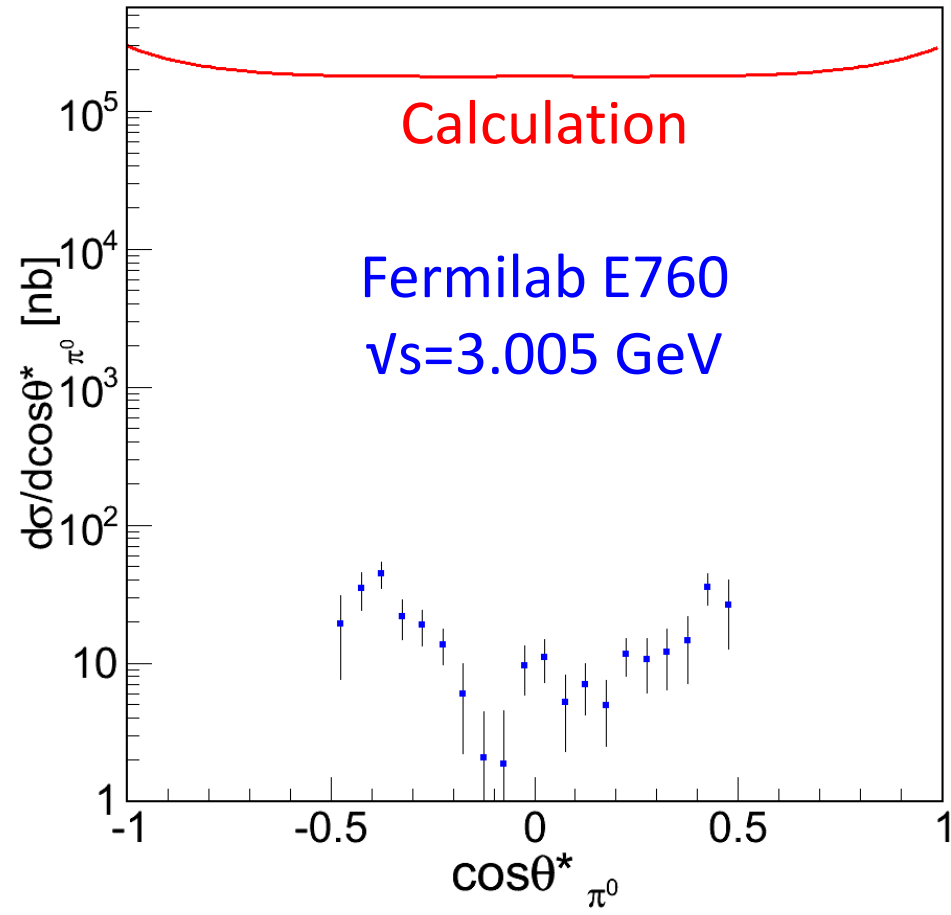
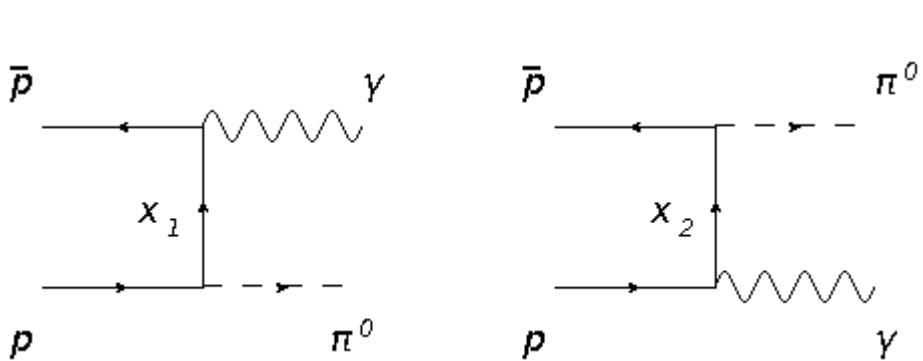
Calculation of $\bar{p}p \rightarrow \pi^0\gamma$

$$d^n\sigma \propto |M|^2 \propto g^{\mu\nu} H_{\mu\nu}(s, \theta_{\pi^0}, G_E(q^2=0), G_M(q^2=0))$$



Calculation of $\bar{p}p \rightarrow \pi^0\gamma$

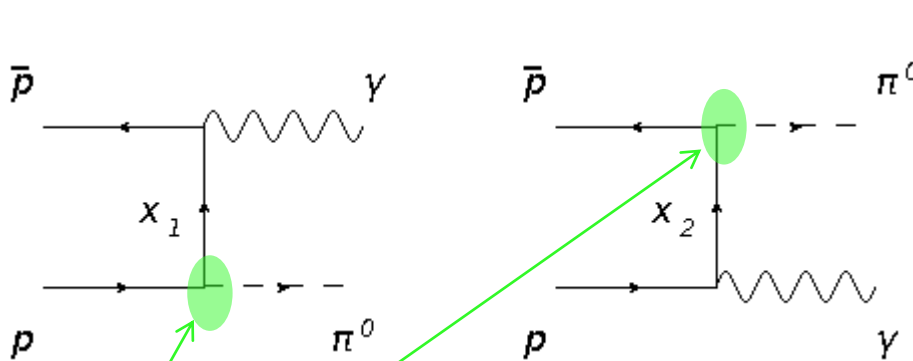
$$d^n\sigma \propto |M|^2 \propto g^{\mu\nu} H_{\mu\nu}(s, \theta_{\pi^0}, G_E(q^2=0), G_M(q^2=0))$$



Calculation by
J. Van de Wiele

Calculation of $\bar{p}p \rightarrow \pi^0\gamma$

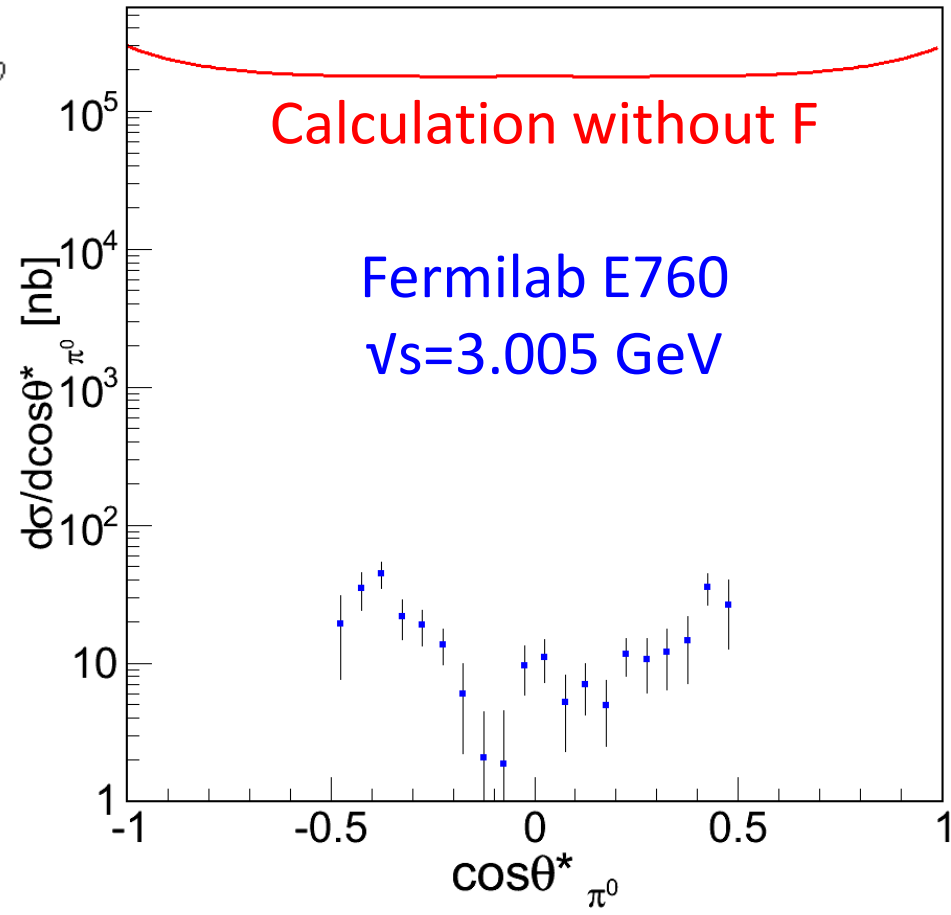
$$d^n\sigma \propto |M|^2 \propto g^{\mu\nu} H_{\mu\nu}(s, \theta_{\pi^0}, G_E(q^2=0), G_M(q^2=0))$$



Hadronic Form factor F :

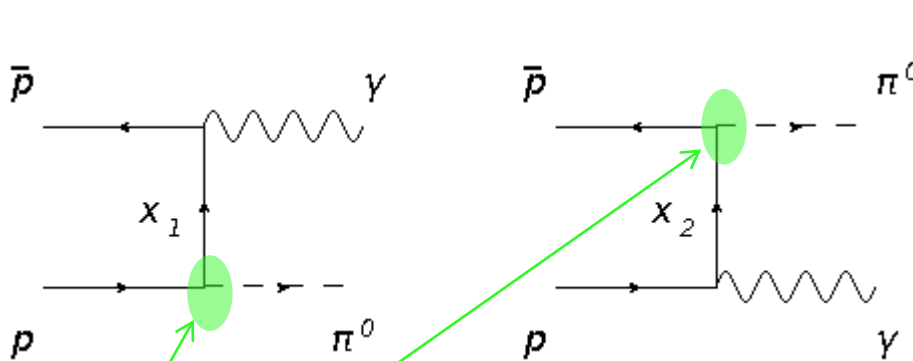
$$F = \sqrt{\left[\frac{\lambda^2 - m_p^2}{\lambda^2 - X_1^2} \right]^2 \left[\frac{\lambda^2 - m_p^2}{\lambda^2 - X_2^2} \right]^2}$$

Calculation by
J. Van de Wiele



Calculation of $\bar{p}p \rightarrow \pi^0\gamma$

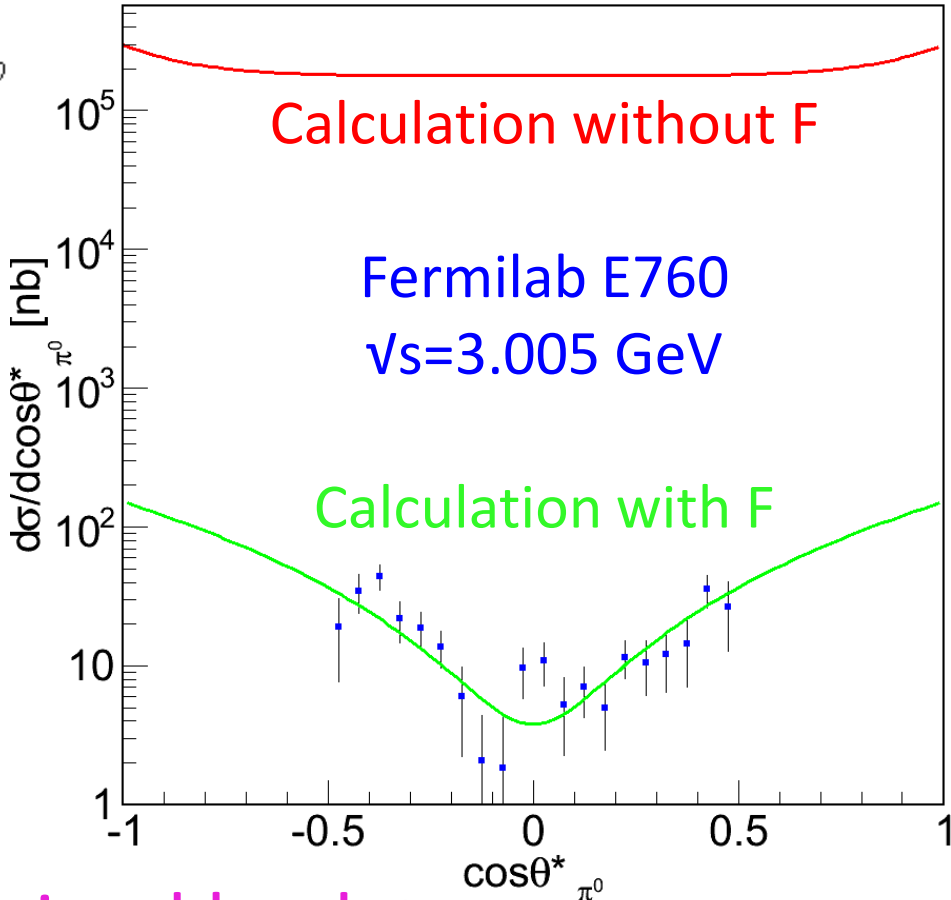
$$d^n\sigma \propto |M|^2 \propto g^{\mu\nu} H_{\mu\nu}(s, \theta_{\pi^0}, G_E(q^2=0), G_M(q^2=0))$$



Hadronic Form factor F:

$$F = \sqrt{\left[\frac{\lambda^2 - m_p^2}{\lambda^2 - X_1^2} \right]^2 \left[\frac{\lambda^2 - m_p^2}{\lambda^2 - X_2^2} \right]^2}$$

Calculation by
J. Van de Wiele



Model constrained by data

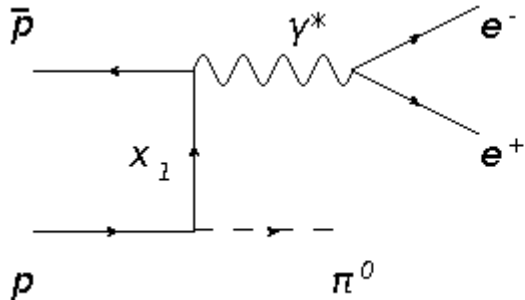
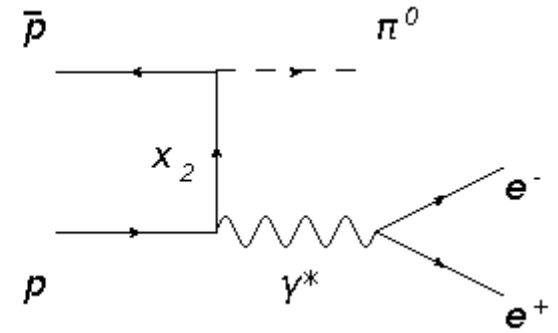
Calculation of $\bar{p}p \rightarrow \pi^0 e^+ e^-$

$$d^n \sigma \propto |M|^2 \propto \frac{1}{q^4} L^{\mu\nu} H_{\mu\nu}(s, q^2, \theta_{\pi^0}, G_E, G_M)$$

In the γ^* rest frame

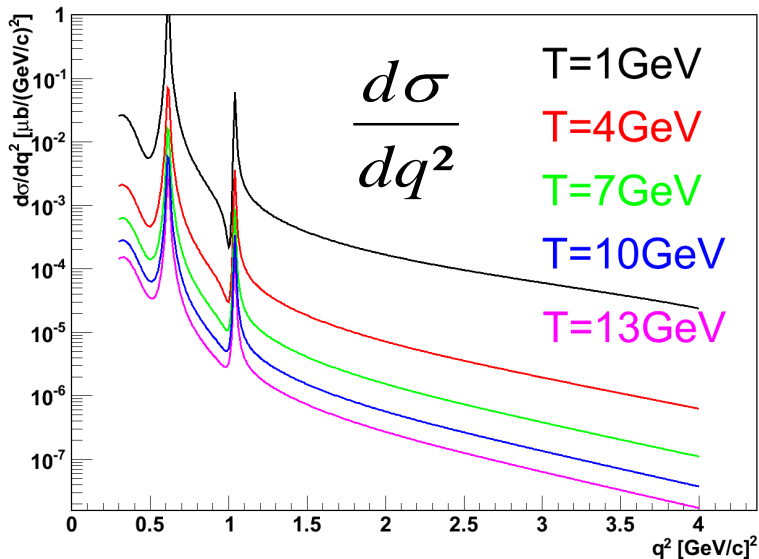
$$L^{\mu\nu} H_{\mu\nu} = 4e^2 \frac{q^2}{2} (H_{11} + H_{22} + H_{33})$$

$$\begin{aligned} & - 8e^2 p_e^2 (H_{11} \sin^2 \theta_e \cos^2 \varphi_e + 2H_{12} \sin^2 \theta_e \sin \varphi_e \cos \varphi_e \\ & + 2H_{13} \sin \theta_e \cos \theta_e \cos \varphi_e + H_{22} \sin^2 \theta_e \sin^2 \varphi_e \\ & + 2H_{23} \sin \theta_e \cos \theta_e \sin \varphi_e + H_{33} \cos^2 \theta_e) \end{aligned}$$



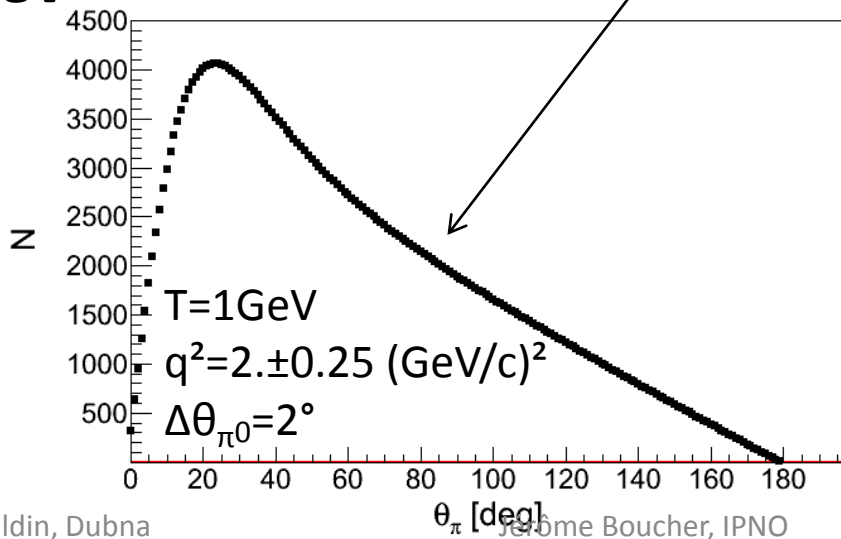
Calculation by
J. Van de Wiele

Dependence on beam kinetic energy

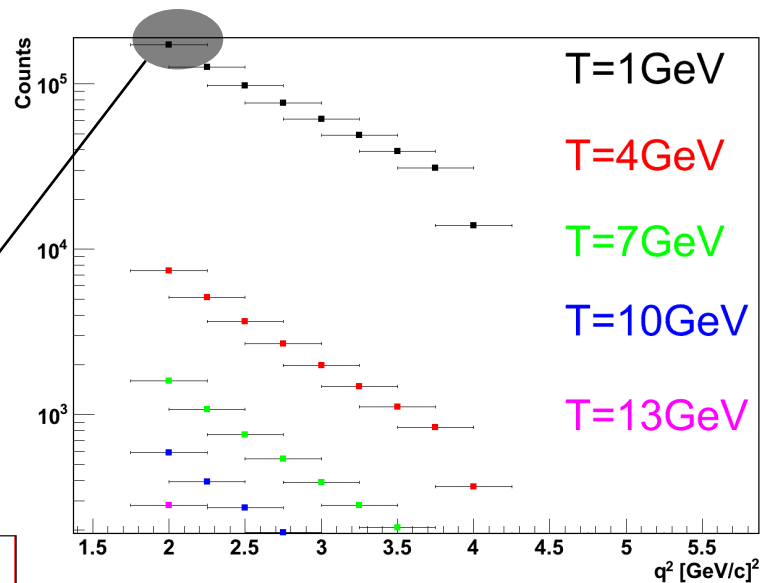


$d\sigma/dq^2$ decreases as T increases.

↳ T=1 GeV



$$\int_{q^2-0.25}^{q^2+0.25} L_{\text{int}} \frac{d\sigma}{dq^2} dq^2$$



Integrated over all π^0 angles.

↳ $q^2 = 2$ (GeV/c)²

$$L_{\text{int}} = 2 \text{ fb}^{-1}$$

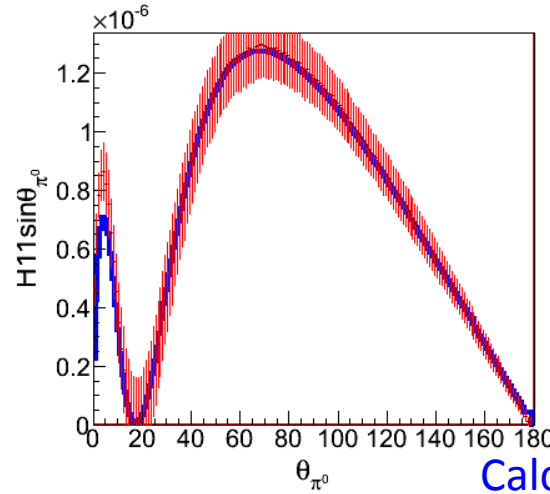
$H_{\mu\nu}$ versus fitted values

- $T=1\text{GeV}$
 - $q^2=2.0 \pm 0.25$
 - $\Delta\theta_{\pi^0}=2^\circ$
- 172 076 events
- For each $\Delta\theta_{\pi^0}$:
 - $d^5\sigma$ is generated with well defined $H_{\mu\nu}$ ($\theta_e, \phi_e:10^\circ/\text{bin}$)
 - $d^5\sigma$ is fitted \rightarrow experimental determination of $H_{\mu\nu}$

$H_{\mu\nu}$ versus fitted values

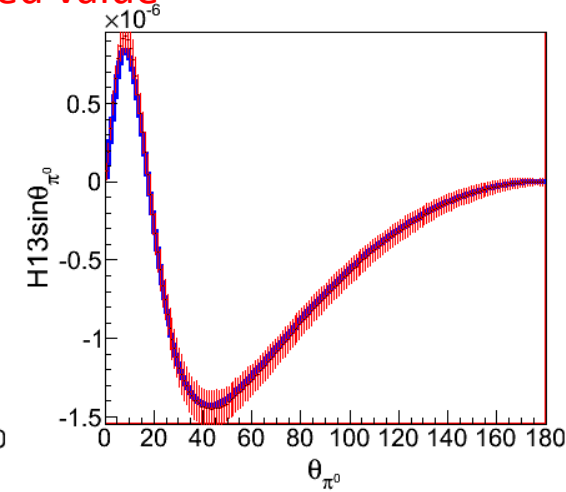
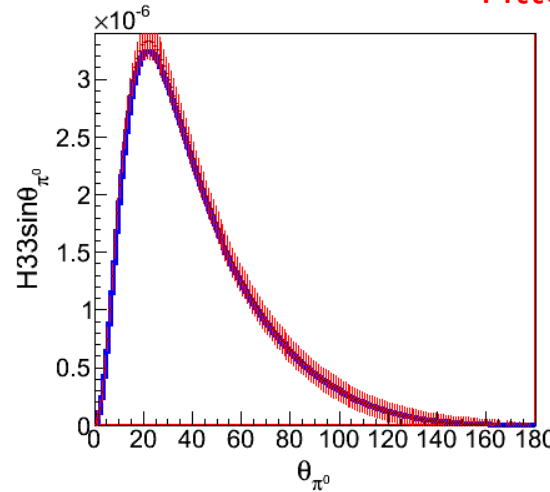
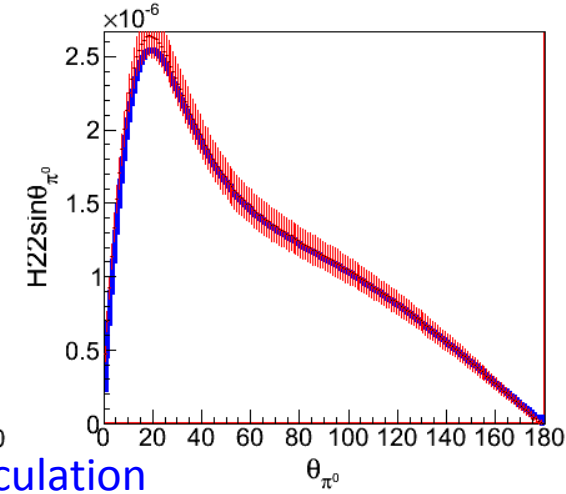
- $T=1\text{GeV}$
- $q^2=2.0 \pm 0.25$
- $\Delta\theta_{\pi^0}=2^\circ$
- For each $\Delta\theta_{\pi^0}$:
 - $d^5\sigma$ is generated with well defined $H_{\mu\nu}$ ($\theta_e, \phi_e:10^\circ/\text{bin}$)
 - $d^5\sigma$ is fitted \rightarrow experimental determination of $H_{\mu\nu}$

172 076 events



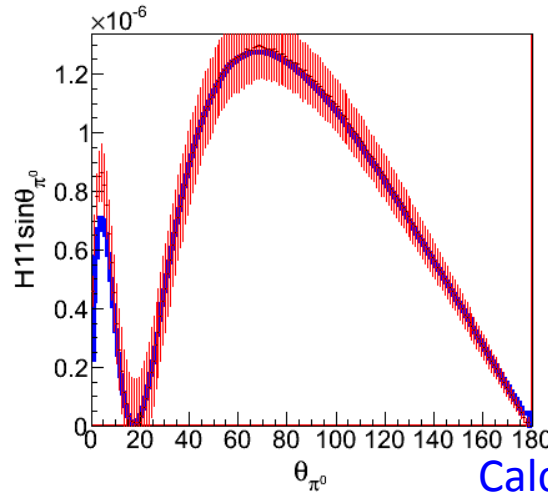
Calculation

Fitted value

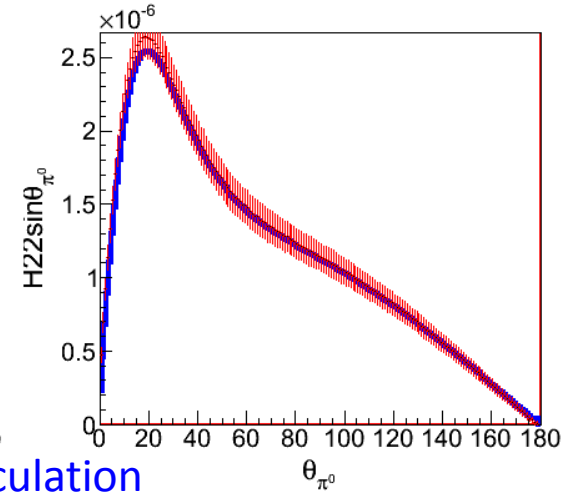


$H_{\mu\nu}$ versus fitted values

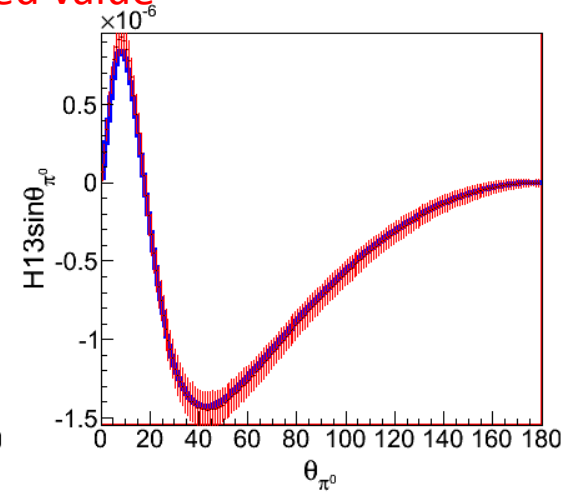
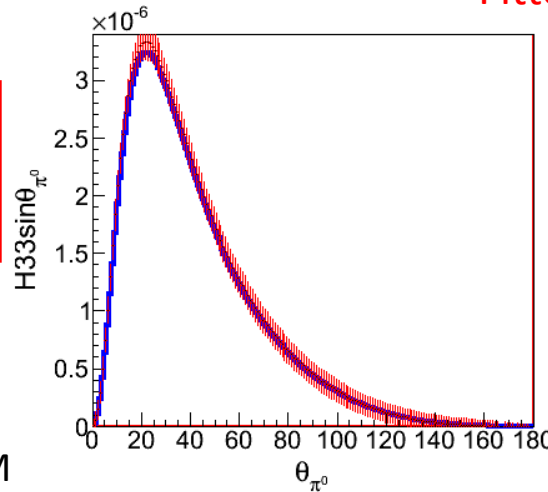
- $T=1\text{GeV}$
 - $q^2=2.0 \pm 0.25$
 - $\Delta\theta_{\pi^0}=2^\circ$
- 172 076 events
- For each $\Delta\theta_{\pi^0}$:
 - $d^5\sigma$ is generated with well defined $H_{\mu\nu}(\theta_e, \phi_e:10^\circ/\text{bin})$
 - $d^5\sigma$ is fitted \rightarrow experimental determination of $H_{\mu\nu}$



Calculation



Fitted value



Direct access to $H_{\mu\nu}$ via the angular distribution



$H_{\mu\nu}$ linked to G_E , G_M , φ_E and φ_M

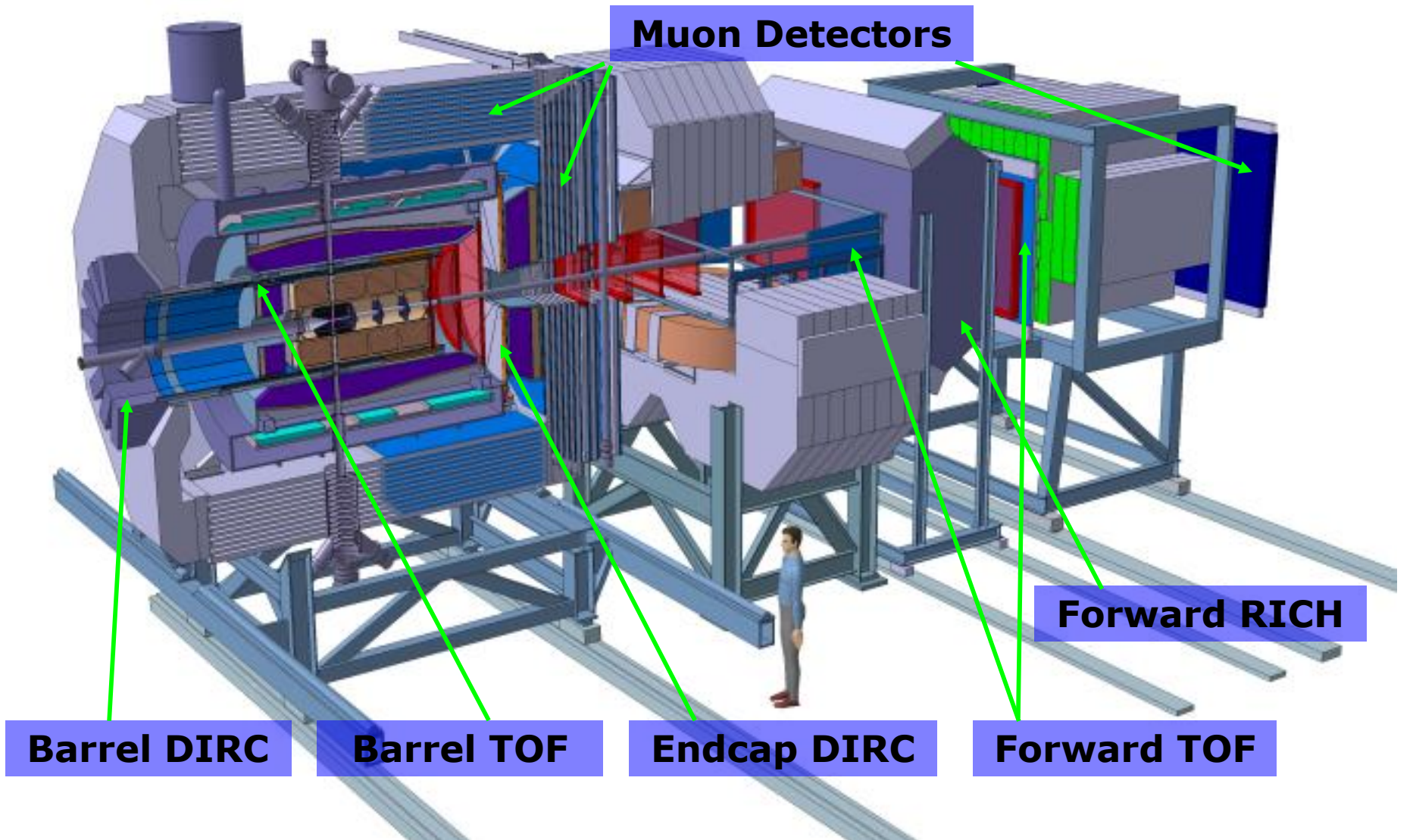


Ratios would provide constraints on $|G_E|/|G_M|$ and $\cos(\varphi_E - \varphi_M)$

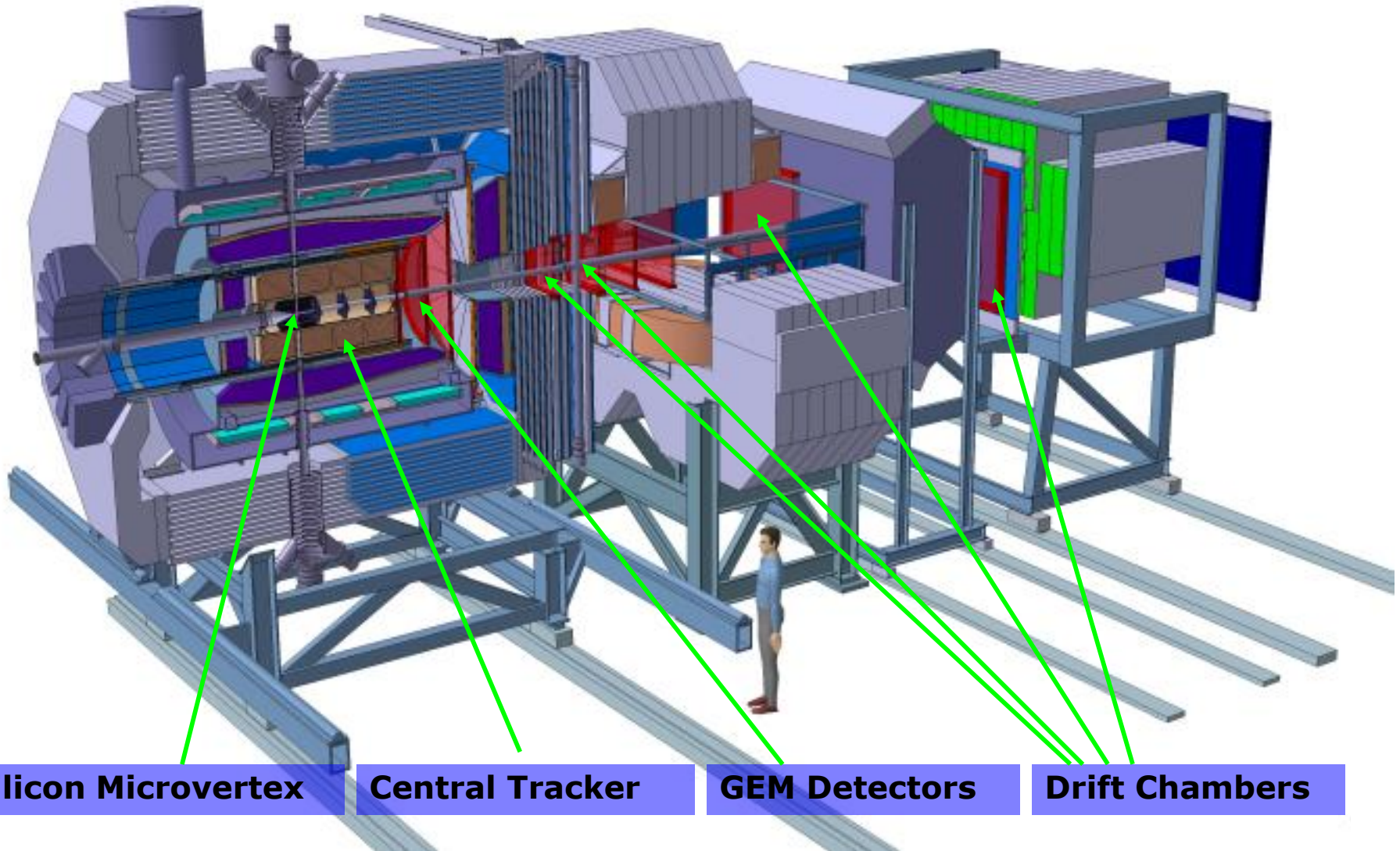
Conclusions and outlook

- \bar{P} ANDA will improve results on $|G_E^{TL}|$ and $|G_M^{TL}|$ by measuring the $\bar{p}p \rightarrow e^+e^-$ angular distributions.
- Realistic model for $\bar{p}p \rightarrow \pi^0 e^+e^-$ in the unphysical region has been developed.
- Access to the hadronic tensors ($H_{\mu\nu}$) is possible via the e^+ (e^-) angular distribution.
 - $|G_E|/|G_M|$ and $\cos(\varphi_E - \varphi_M)$.
- Feasibility of $\bar{p}p \rightarrow \pi^0 e^+e^-$ and background suppression under investigation.
- See E. Tomasi-Gustafsson talk (s-channel)

Detectors for charged particle identification



Tracking detectors



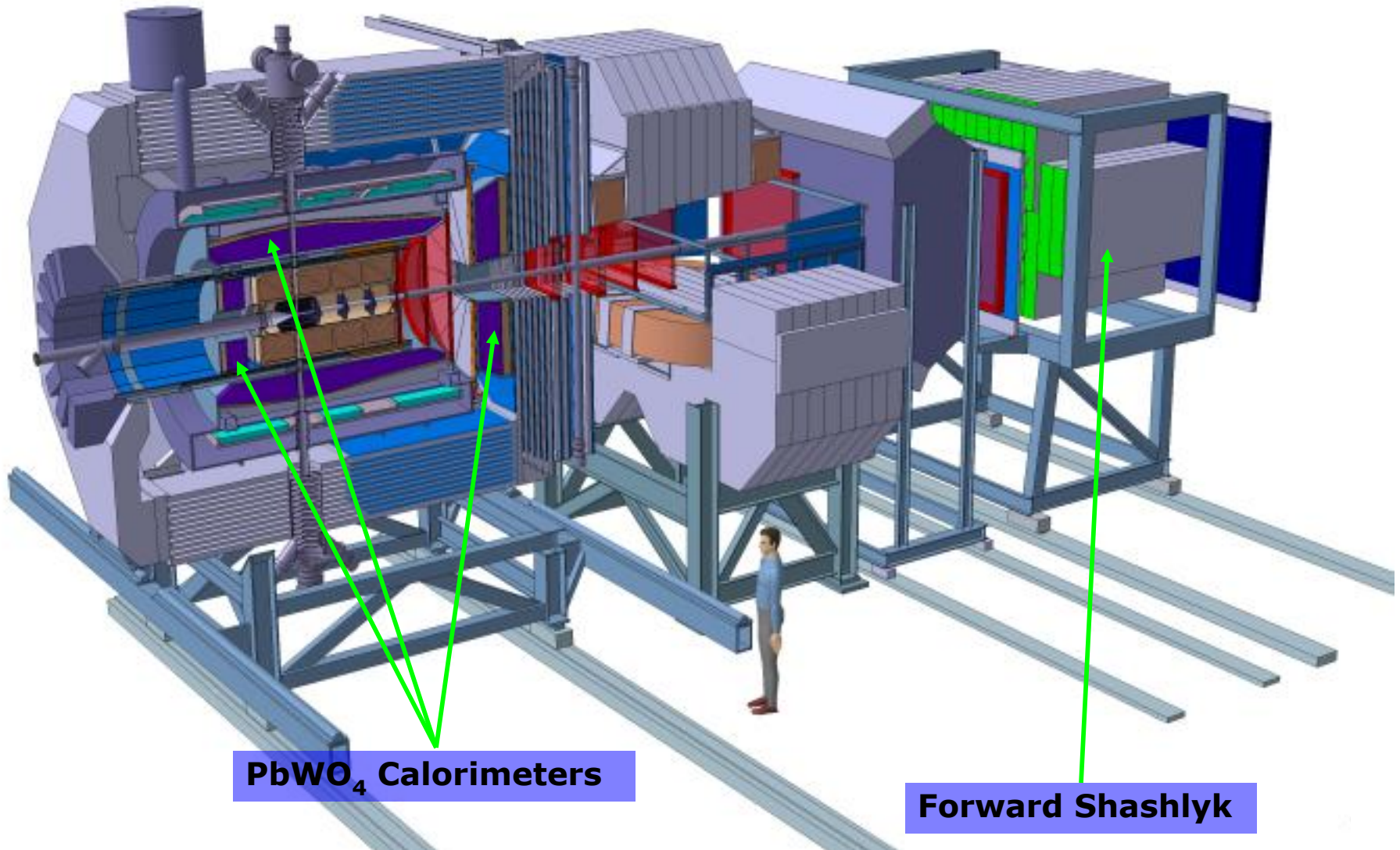
Silicon Microvertex

Central Tracker

GEM Detectors

Drift Chambers

PANDA calorimeters



General information of the simulation

q^2	e^+e^-	$\pi^+\pi^-$	$\pi^0\pi^0$
[(GeV/c) ²]			
5.4	$4 \cdot 10^6$	$1 \cdot 10^8$	$3 \cdot 10^6$
7.21	$4 \cdot 10^6$	-	-
8.21	$4 \cdot 10^6$	-	-
12.9	$4 \cdot 10^6$	$1 \cdot 10^8$	$3 \cdot 10^6$
13.9	$4 \cdot 10^6$	-	-
16.7	$4 \cdot 10^6$	$2 \cdot 10^8$	$3 \cdot 10^6$
22.3	$4 \cdot 10^6$	-	-

Signal has been simulated under 3 assumptions:

- $|G_E| = 0$
- $|G_E| = |G_M|$
- $|G_E| = 3 |G_M|$

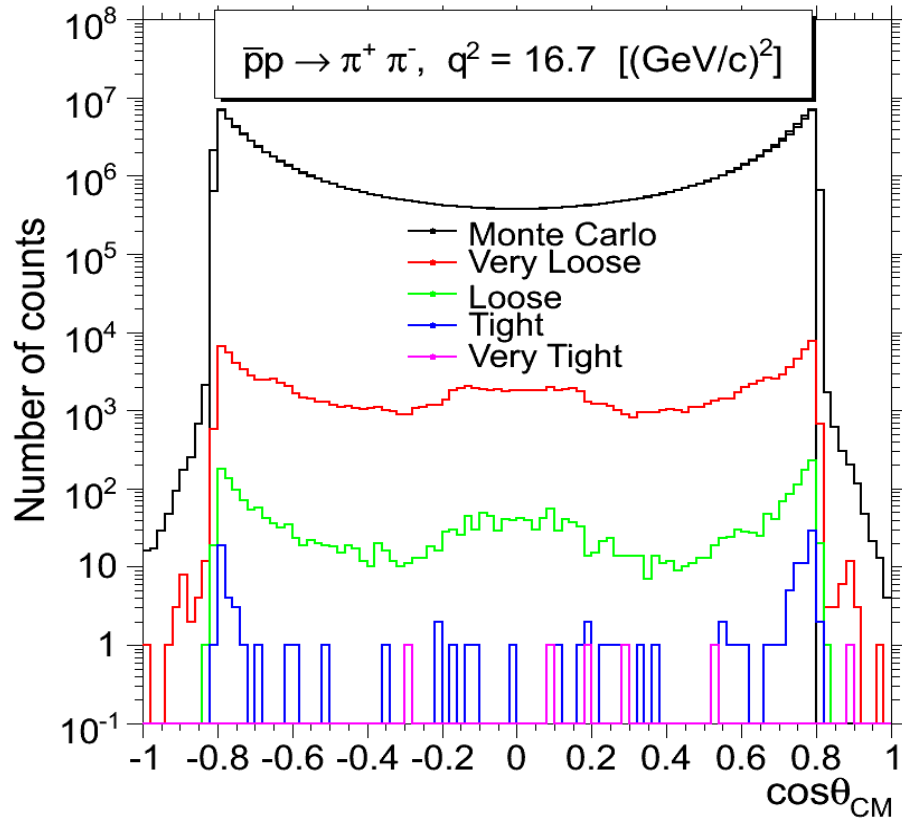
3 scenarios for the π^0 decay were taken into account

- $\pi^0\pi^0 \rightarrow \gamma\gamma\gamma\gamma$
- $\pi^0\pi^0 \rightarrow \gamma\gamma\gamma e^+e^-$
- $\pi^0\pi^0 \rightarrow \gamma e^+e^- \gamma e^+e^-$

γ – convert in the detector material

- Full scale simulation including GEANT4 and detector digitalization ,
- Both the signal $\bar{p} p \rightarrow e^+ e^-$ and main background channel $\bar{p} p \rightarrow \pi^+ \pi^-$ analysed,
- Detailed analysis for the PID response and also kinematic constraints were studied.

Hadronic background channel suppression



Background suppression factor is at least of the order of 10^9 taking into account PID & kinematic fit !!

Definition of the PID cuts:
(particle probability of being an electron)

Very Loose : 19.9%
Loose : 85%
Tight : 99%
Very Tight : 99.8 %

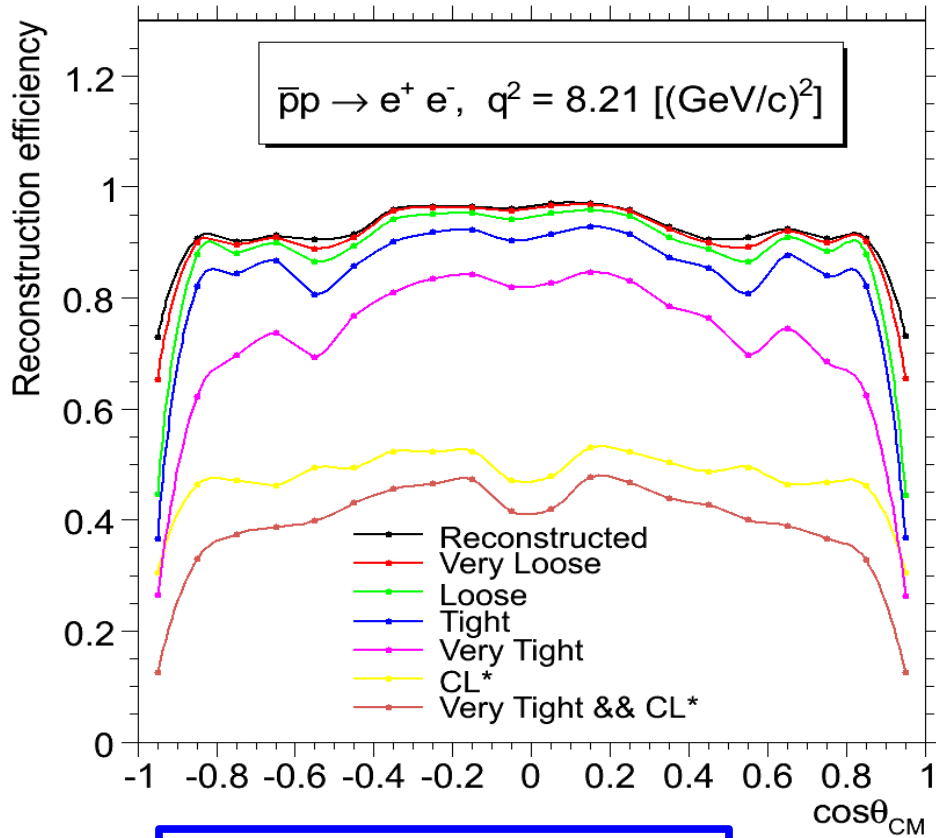
PID from 5 detectors:
EMC, STT, DIRC, MVD and MUO

Background suppression after
Very Tight PID cuts:

- 8.2 (GeV/c)² : $2/10^8$
- 12.9 (GeV/c)² : $5/10^8$
- 16.7 (GeV/c)² : $6/10^8$

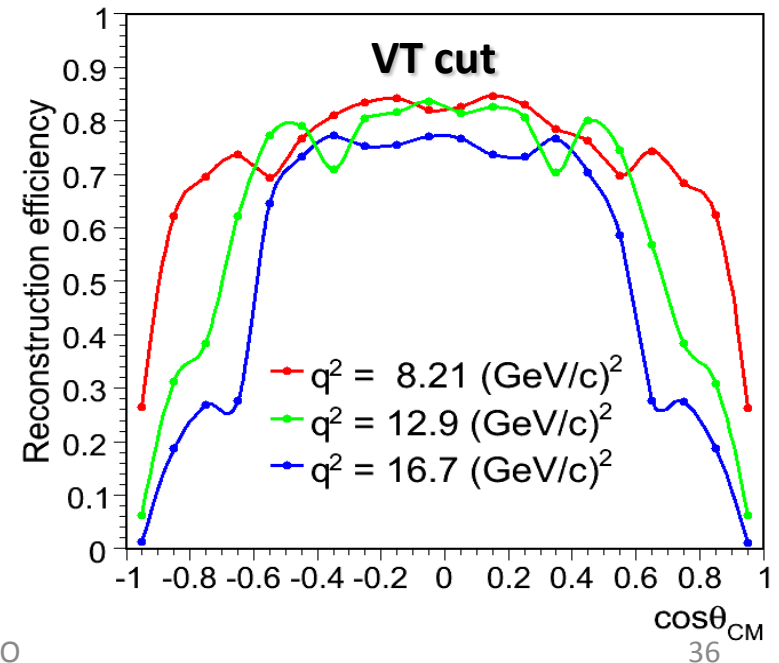
Additional factor ~ 100 applying the kinematic fit

Electron reconstruction efficiency



- e^+e^- signal:**
- efficiency about 35 % at $\cos\theta_{CM}=0$ after all cuts (Very Tight and CL*)
 - decreases at forward/backward angles (combined effect with acceptance)
 - more pronounced for the high q^2
 - still on average a factor 2 higher than BABAR experiment ($\varepsilon \sim 17 \%$)

q^2 [GeV/c] ²	$\pi^+\pi^-$ contamination
8.2	0.004 %
12.9	0.017 %
16.7	0.061 %



2-dimensional fits

Default parameters:

- Chi-square method
- Empty bins are ignored
- Error = $\sqrt{\text{bin content}}$

Options:

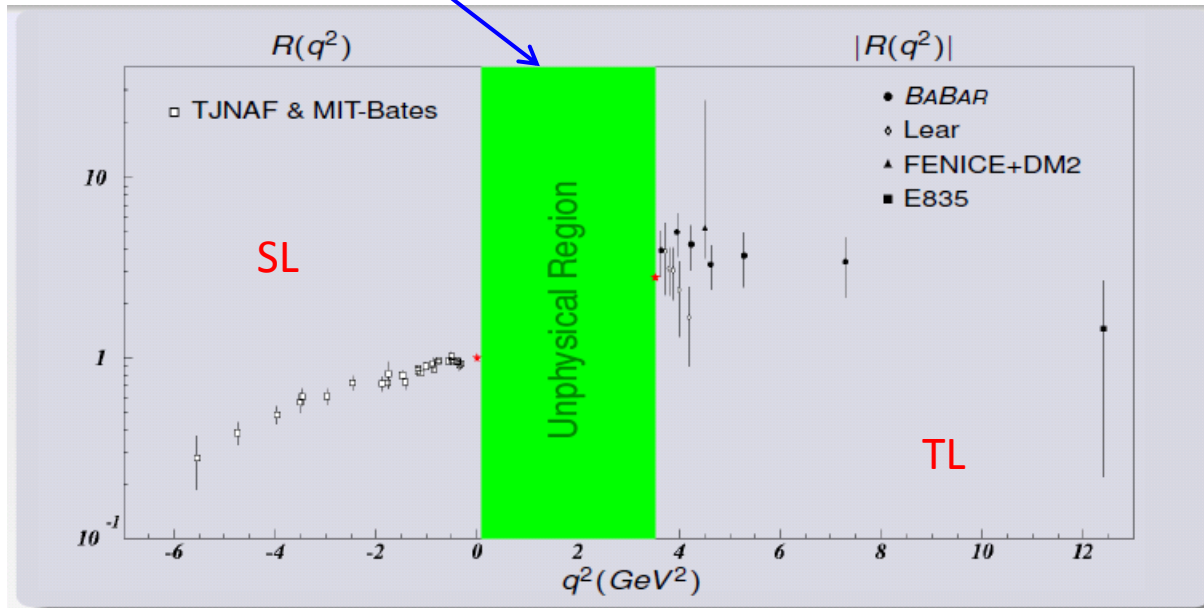
- W: Set weight to 1 for non empty bins
- WW: Set weight to 1 for all bins
- I: Integral of function instead of value at bin center
- ...

Form factors and unphysical region

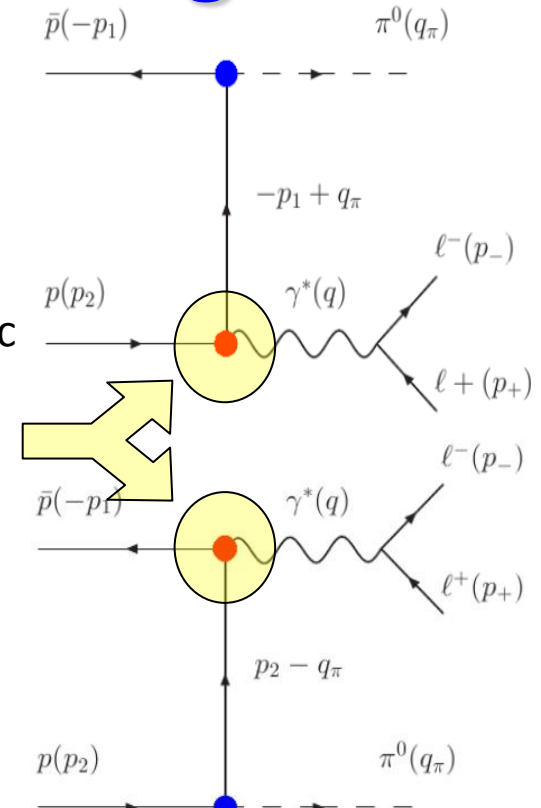
Motivations:

Access to the unphysical region,
 $(q^2 < 4m_p^2)$ via reaction:

Never measured.



Electromagnetic
Form Factors



★ Theoretical constraints ★

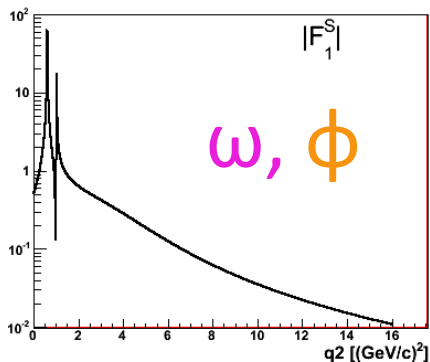
$$R(0) = 1 \quad R(4M_N^2) = \mu_p$$

$$R = \mu_p G_E^p / G_M^p$$

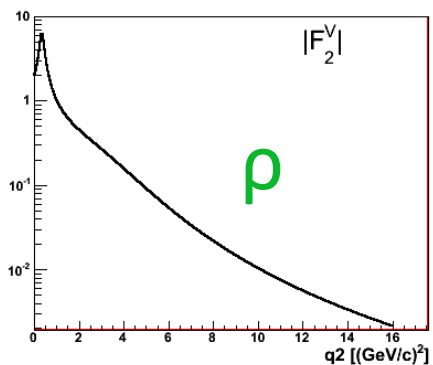
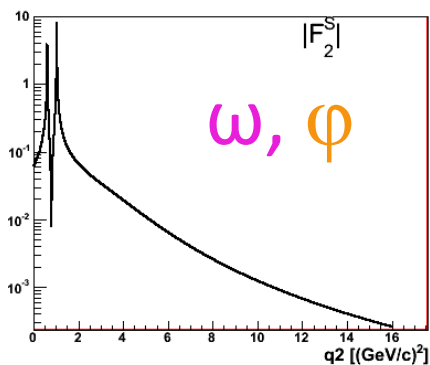
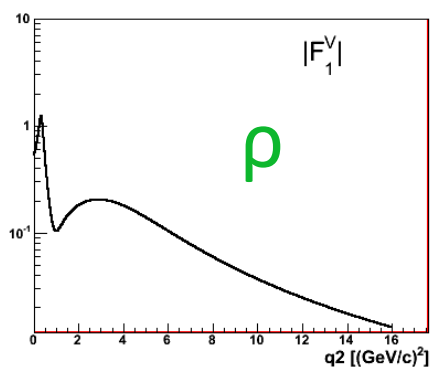
By Simone Pacetti
GDR Nucleon Meeting

Iachello's Form Factors

Isoscalar

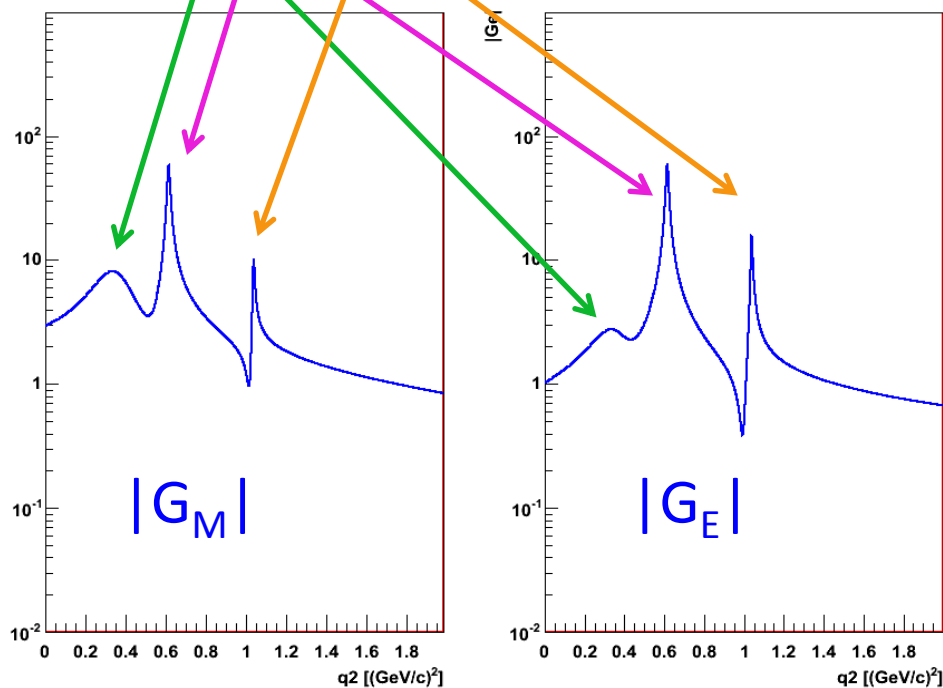


Isovector



Vector Meson Dominance (VMD):

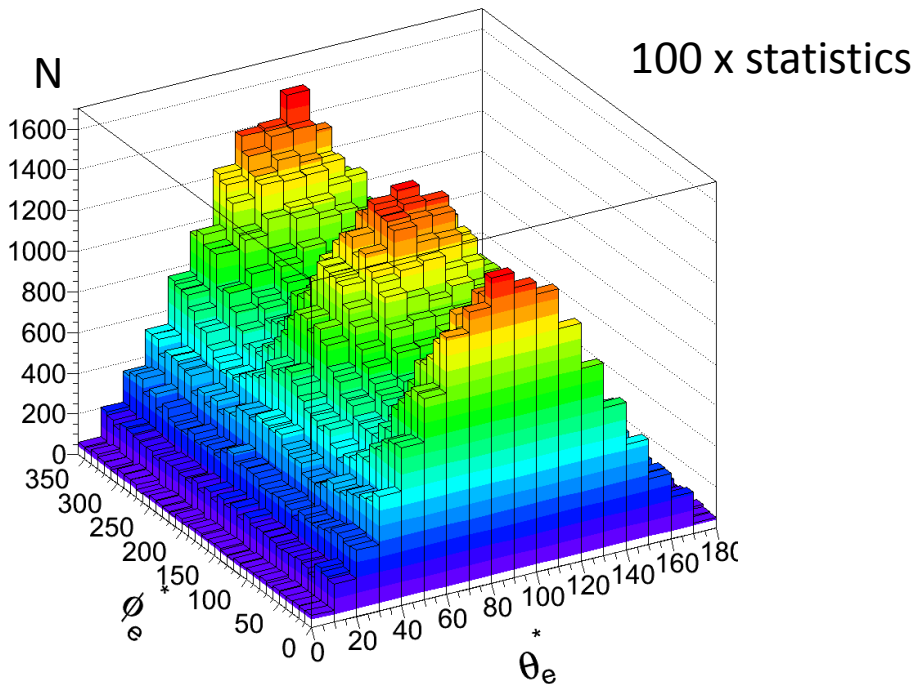
ρ , ω and ϕ



(F. Iachello, Phys. Rev. C 69, 055204, 2004)

$H_{\mu\nu}$ versus fitted values

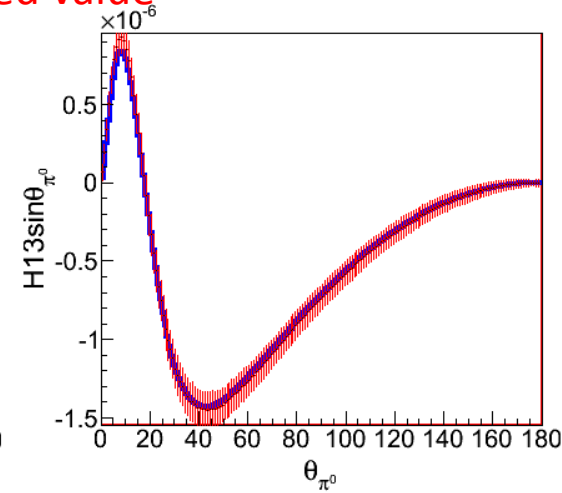
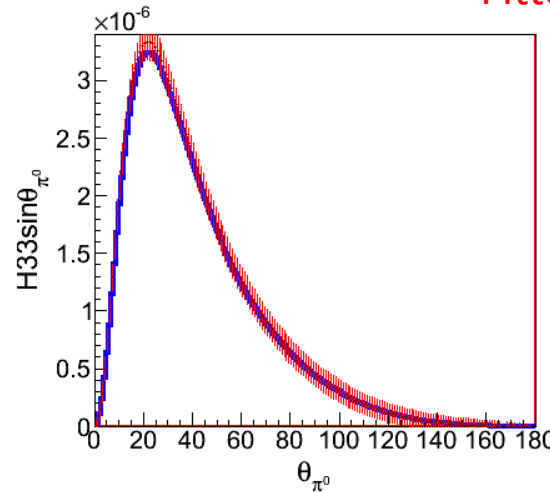
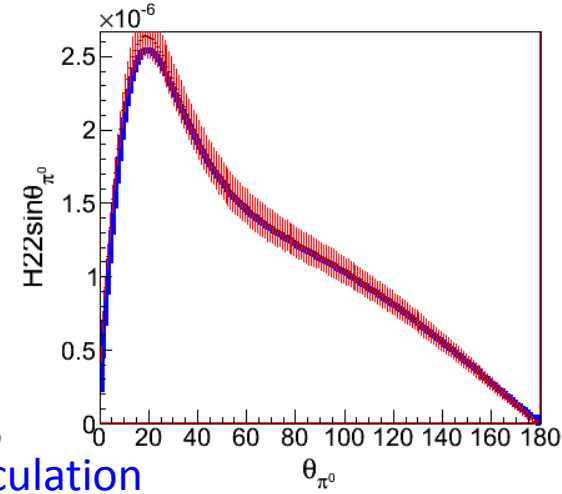
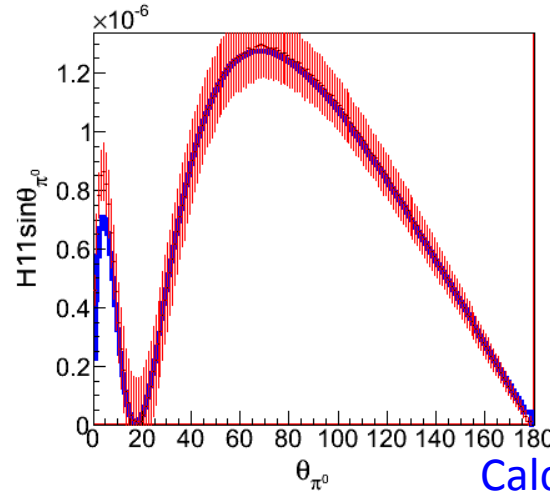
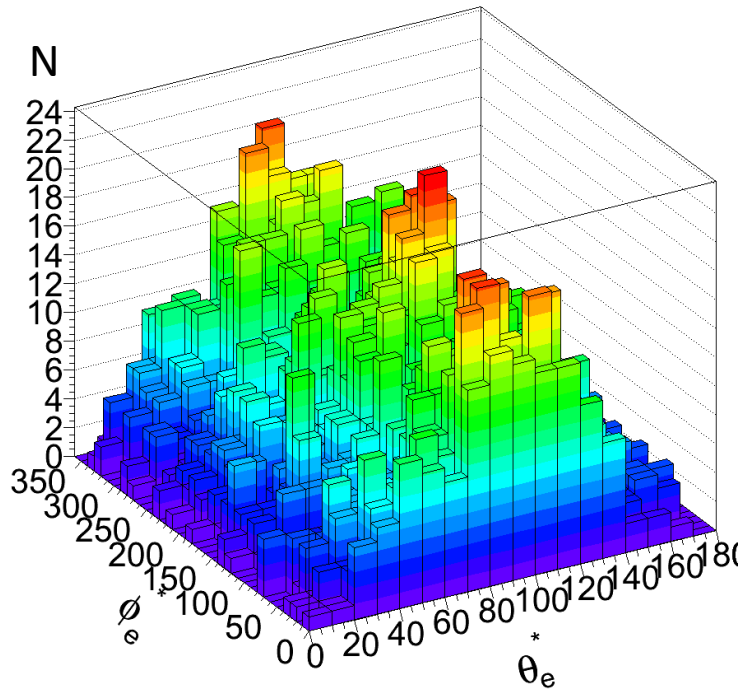
- $T=1\text{GeV}$
 - $q^2=2.0 \pm 0.25$
- 172 076 events
- For each θ_{π^0} (θ_e, ϕ_e : 10° per bin):
 - $d^5\sigma$ is generated
 - $d^5\sigma$ is fitted



Direct access to H_{ij} via the angular distribution

$H_{\mu\nu}$ versus fitted values

- $T=1\text{GeV}$
- $q^2=2.0 \pm 0.25$
- For each θ_{π^0} (θ_e, ϕ_e : 10° per bin):
 - $d^5\sigma$ is generated
 - $d^5\sigma$ is fitted



Calculation

Fitted value

Direct access to H_{ij} via the angular distribution